The Lucas Orchard

Ian Martin*

26 November, 2008

Abstract

I solve for asset prices, expected returns, and the term structure of interest rates in an endowment economy in which a representative agent with power utility consumes the dividends of multiple assets. The assets are Lucas trees; a collection of Lucas trees is a Lucas orchard. The model replicates various features of the data. Assets with independent dividends exhibit comovement in returns. Disasters spread across assets. Assets with high price-dividend ratios have low risk premia. Small assets exhibit momentum. High yield spreads forecast high excess returns on bonds and on the market. Special attention is paid to the behavior of very small assets, which may comove endogenously and hence earn positive risk premia even if their fundamentals are independent of the rest of the economy. Under plausible conditions, the variation in a small asset's price-dividend ratio is entirely due to variation in its risk premium.

*ian.martin@stanford.edu; http://www.stanford.edu/∼iwrm/. First draft: 9 October 2006. I thank Tobias Adrian, Malcolm Baker, Thomas Baranga, Robert Barro, John Cochrane, George Constantinides, Josh Coval, Emmanuel Farhi, Xavier Gabaix, Lars Hansen, Jakub Jurek, David Laibson, Robert Lucas, Greg Mankiw, Emi Nakamura, Martin Oehmke, Lubos Pastor, Roberto Rigobon, David Skeie, Jon Steinsson, Aleh Tsyvinski, Harald Uhlig, Pietro Veronesi, Luis Viceira, James Vickery, and Jiang Wang for their comments. I am particularly grateful to John Campbell and Chris Rogers for their advice.

This paper is a theoretical exercise motivated by a well-documented empirical fact: across different countries' stock markets, there is more comovement in returns than in fundamentals (Shiller (1989), Ammer and Mei (1996)). It investigates the properties of asset prices, risk premia, and the term structure of interest rates in a continuous-time economy in which a representative agent with power utility consumes the sum of the dividends of N assets. The assets can be thought of as Lucas trees, so I call the collection of assets a Lucas orchard. An individual asset, or tree, represents a particular country's stock market.[1]

Each of the assets is assumed to have i.i.d. dividend growth over time, though there may be correlation between the dividend growth rates of different assets. Formally, the vector of log dividends follows a Lévy process. This framework allows for the case in which dividends follow geometric Brownian motions, but also allows for a rich structure of jumps in dividends. Standard lognormal models make poor predictions for key asset-pricing quantities such as the equity premium and riskless rate (Mehra and Prescott (1985)), and recently there has been increased interest in models which allow for the possibility of disasters (Rietz (1988), Barro (2006), Gabaix (2008)). By allowing for jumps, I avoid these puzzles without relying on implausible levels of risk aversion or dividend volatility. Introducing jumps also allows me to address a high-profile example of comovement, namely disasters that spread across markets.

Despite its simple structure, the model exhibits surprisingly rich asset price behavior, including several phenomena that have been documented in the empirical literature; it illustrates "the importance of explicit recognition of the essential interdependences of markets in theoretical and empirical specifications of financial models" (Brainard and Tobin (1968)).

At one level, it is the interaction between multiplicative structure (induced by i.i.d. growth in log dividends) and additive structure (consumption is the sum of dividends) that makes the model hard to solve. I use techniques from complex analysis to solve for prices, returns, and interest rates in terms of integral formulas that can be evaluated numerically, subject to conditions that ensure finiteness of asset prices, and hence of the representative agent's expected utility. When there are two assets whose dividends follow geometric Brownian motions, the integrals can be solved in closed form.

In the general case considered here, dividends—and hence prices, expected returns, and interest rates—can jump, and neither the conditional consumption-CAPM

[1] In other applications, a tree might represent a particular industry or asset class.

(Breeden (1979)) nor the ICAPM (Merton (1973)) hold. In the special case in which dividends follow geometric Brownian motions, asset prices follow diffusions; then, the ICAPM and conditional consumption-CAPM do hold.[2] Here, though, price processes are not taken as given but are determined endogenously based on exogenous fundamentals, in the spirit of Cox, Ingersoll and Ross (1985).

The tractability of the model in the general i.i.d. case is due in part to the use of cumulant-generating functions (CGFs). Martin (2008) expresses the riskless rate, risk premium, and consumption-wealth ratio in terms of the CGF in the case $N = 1$, and the expressions found there are echoed in the more complicated scenario considered here. In effect, working with CGFs makes the mathematics no harder than when working with lognormal models; the advantage of doing so is that one then "gets jumps for free". In fact, the use of CGFs may even make things *simpler* because one can follow the CGF's progress through the algebra: the mathematical equivalent of a barium meal! Furthermore, CGFs have useful properties that I use in various proofs.

For simplicity, I introduce the model in the case $N = 2$. I present two calibrations, each intended to highlight different features of the model. In the first, dividends follow geometric Brownian motions. In the second, I use a calibration based on Barro (2006) to explore the impact of rare disasters in a multi-asset framework.

The model generates price comovement even between assets whose dividends are independent. To see why this happens, suppose that one asset's price increases as a result of a positive shock to dividends. The other asset now contributes a smaller proportion of overall consumption, and therefore typically has a lower required return and hence a higher price.[3] Such comovement is a feature of the data. Shiller (1989) demonstrates that stock prices in the US and UK move together more closely than do fundamentals; Forbes and Rigobon (2002) allow for heteroskedasticity in returns and find consistently high levels of interdependence between markets.

The riskless rate varies over time, so the term structure of interest rates is not flat. The term structure can be upward-sloping, downward-sloping or hump-shaped (with medium-term bonds earning higher yields than short- and long-term bonds). When the term structure slopes up—the more usual case in the scenarios I consider—long-term bonds earn positive risk premia. High yield spreads forecast high excess returns

[2]The conditional CAPM itself holds only if dividends follow geometric Brownian motions and the representative agent has log utility, as in Cochrane, Longstaff and Santa-Clara (2008).

[3]In some circumstances, discussed further below, movements in the riskless rate may partially offset or reverse this effect.

on the market and on long-term bonds (Fama and French (1989)).

In the second calibration, occasional disasters afflict the two assets. The phenomena described above are present, and there are now some new features. First, the introduction of disasters enables the calibration, like that of Barro (2006), to avoid the equity premium and riskless rate puzzles. Second, disasters spread across assets. When a large asset experiences a disaster, the price of the other (small) asset also jumps downwards. This corresponds to the "typical" case of comovement described above. When, on the other hand, a very small asset suffers a disaster, interest rates drop and the other (large) asset's price jumps *up*. I label these phenomena "contagion" and "flight-to-quality".

Contagion effects provide a new channel through which disasters can contribute to high risk premia. For example, suppose that asset 1 has perfectly stable dividends, but that asset 2 is subject to occasional disastrous declines in dividends. Contagion leads to declines in the price of asset 1 at times when asset 2 experiences a disaster. These occasional price drops may induce a substantial risk premium in asset 1, an ostensibly perfectly safe asset.

I next consider the limit in which one of the two assets is negligibly small by comparison with the other. This case is of special interest because it represents the most extreme departure from simple models in which price-dividend ratios are constant, and crystallizes the distinctive features of the model. Closed-form solutions are available, and an unexpected phenomenon emerges.

To illustrate this, suppose that the two assets have independent dividend streams. Intuition suggests that a small idiosyncratic asset earns no risk premium, that its expected return is therefore equal to the riskless rate and that it can be valued using a Gordon growth formula; in other words, its dividend yield should equal the riskless rate minus expected dividend growth. I show that this intuition is correct whenever the result of the calculation is meaningful, which is to say positive. What happens if the riskless rate (determined by the characteristics of the large asset) is less than the mean dividend growth of the small asset? I show that the negligibly small asset then has a well-defined price-consumption ratio that, as one would expect, tends to zero in the limit. It has, however, an extremely high valuation in the sense that its price-dividend ratio is infinite in the limit. This valuation effect is reminiscent of, and complementary to, that present in the papers of Pástor and Veronesi (2003, 2006). Despite its independent fundamentals and negligible size, such an asset comoves endogenously, and hence earns a positive risk premium. In the general case, I provide a precise characterization of when the Gordon growth model does and does not work, and solve for limiting expected returns and price-dividend ratios in closed form.

I also derive simple closed-form approximations for the price-dividend ratio, riskless rate and expected excess return on the small asset that are valid *near* the small-asset limit. Time variation in the dividend share of the small asset induces time variation in its price-dividend ratio, in its expected excess return, and in the riskless rate. Under certain conditions, variation in the small asset's price-dividend ratio can be attributed to variation in its expected *excess* return: variation in the riskless rate is negligible by comparison. This is tantalizingly reminiscent of a feature of the data emphasized by Cochrane (2005, p. 400).

The final section extends the analysis to N assets. I argue that positive comovement (contagion) is a more robust phenomenon than negative comovement (flight-to-quality). I also connect with the empirical work of Ammer and Mei (1996) by carrying out Monte Carlo simulations of a three-asset economy, the three assets representing the stock markets of the US, UK, and the rest of the world. In the model, as in the data, there is more cross-country correlation in discount-rate news than in cashflow news (in the terminology of Campbell (1991)), and US cashflow news is negatively correlated with UK discount rate news while UK cashflow news is positively correlated with US discount-rate news.

Various authors have investigated related models. Cole and Obstfeld (1991) explore the welfare gains from international risk sharing. Brainard and Tobin (1992, section 8) investigate a two-asset model in which per-period endowments are specified by a Markov chain with a small number of states. They present limited numerical results, and—after noting that their "model is simple and abstract; nevertheless it is not easy to analyze"—no analytical results. Menzly, Santos and Veronesi (2004) and Santos and Veronesi (2006) present models in which the dividend shares of assets are assumed to follow mean-reverting processes. By picking convenient functional forms for these processes, closed-form pricing formulas are available. Pavlova and Rigobon (2007) investigate an international asset pricing model, but impose log-linear preferences so price-dividend ratios are constant.

A more closely related paper is that of Cochrane, Longstaff and Santa-Clara (2008), who solve a model in which a representative investor with log utility consumes the dividends of two assets whose dividend processes follow geometric Brownian motions. My solution technique is entirely different, and permits me to allow for power utility, for jumps in dividends, for $N \geq 2$ assets, and to give a complete description of the behavior of a small asset in the $N = 2$ case. I also solve for bond yields, and hence expand the set of predictions made by the model.

1 Setup

For the time being, I restrict to the two-asset case for clarity. Setting the model up amounts to making *technological* assumptions about dividend processes; making assumptions about the *preferences* of the representative investor that, together with consumption, pin down the stochastic discount factor; and closing the model by specifying that the representative investor's consumption is equal to the sum of the two assets' dividends.

1.1 The stochastic discount factor

Time is continuous, and runs from 0 (the present) to infinity. I assume that there is a representative agent with power utility over consumption C_t, with coefficient of relative risk aversion γ (a positive integer) and time preference rate ρ. The Euler equation, derived by Lucas (1978) and applied in the two-country context by Lucas (1982), states that the price of an asset with dividend stream $\{X_t\}$ is

$$P_X = \mathbb{E} \int_0^\infty e^{-\rho t} \left(\frac{C_t}{C_0} \right)^{-\gamma} \cdot X_t \, dt \, . \tag{1}$$

1.2 Dividend processes

The two assets, indexed $i = 1, 2$, throw off random dividend streams D_{it}. Dividends are positive, which makes it natural to work with log dividends, $y_{it} \equiv \log D_{it}$. At time 0, the dividends (y_{10}, y_{20}) of the two assets are arbitrary. The vector $\widetilde{\boldsymbol{y}}_t \equiv \boldsymbol{y}_t - \boldsymbol{y}_0 \equiv (y_{1t} - y_{10}, y_{2t} - y_{20})$ is assumed to follow a Lévy process.[4] This is the continuous-time analogue of the discrete-time assumption that dividend growth is i.i.d. In the special case in which $\widetilde{\boldsymbol{y}}$ is a jump-diffusion, we can write

$$\boldsymbol{y}_t = \boldsymbol{y}_0 + \boldsymbol{\mu} t + \boldsymbol{A} \boldsymbol{Z}_t + \sum_{k=1}^{N(t)} \boldsymbol{J}^k \, . \tag{2}$$

Here $\boldsymbol{\mu}$ is a two-dimensional vector of drifts, $\boldsymbol{A}$ a 2×2 matrix of factor loadings, $\boldsymbol{Z}_t$ a 2-dimensional Brownian motion, $N(t)$ a Poisson process with arrival rate ω that

[4] See Sato (1999) for a comprehensive treatment of Lévy processes.

represents the number of jumps that have taken place by time t, and $\boldsymbol{J}^k$ are two-dimensional random variables which are distributed like the random variable $\boldsymbol{J}$, and which are assumed to be i.i.d. across time. The covariance matrix of the diffusion components of the two dividend processes is $\boldsymbol{\Sigma} \equiv \boldsymbol{A}\boldsymbol{A}'$, whose elements I write as σ_{ij}.

The following definition introduces an object which turns out to capture all relevant information about the stochastic processes driving dividend growth.

Definition 1. *The* cumulant-generating function $\boldsymbol{c}(\boldsymbol{\theta})$ *is defined by*

$$\boldsymbol{c}(\boldsymbol{\theta}) \equiv \log \mathbb{E} \exp \boldsymbol{\theta}'(\widetilde{\boldsymbol{y}}_{t+1} - \widetilde{\boldsymbol{y}}_t) \,. \tag{3}$$

Since Lévy processes have i.i.d. increments, $\boldsymbol{c}(\boldsymbol{\theta})$ is independent of t.

Some conditions on the Lévy process $\widetilde{\boldsymbol{y}}$ are required to ensure that asset prices are finite; these are discussed further below. In particular, I need the CGF to exist in an appropriate open set containing the origin.

If log dividends follow a jump-diffusion as in (2), then $\boldsymbol{c}(\boldsymbol{\theta}) = \boldsymbol{\theta}'\boldsymbol{\mu} + \boldsymbol{\theta}'\boldsymbol{\Sigma}\boldsymbol{\theta}/2 + \omega\left(\mathbb{E}e^{\boldsymbol{\theta}'\boldsymbol{J}} - 1\right)$. If the jump sizes are Normally distributed, $\boldsymbol{J} \sim N(\boldsymbol{\mu}_J, \boldsymbol{\Sigma}_J)$, then

$$\boldsymbol{c}(\boldsymbol{\theta}) = \boldsymbol{\theta}'\boldsymbol{\mu} + \frac{1}{2}\boldsymbol{\theta}'\boldsymbol{\Sigma}\boldsymbol{\theta} + \omega\left(\exp\left\{\boldsymbol{\theta}'\boldsymbol{\mu}_J + \frac{1}{2}\boldsymbol{\theta}'\boldsymbol{\Sigma}_J\boldsymbol{\theta}\right\} - 1\right) .$$

1.3 Closing the model

Dividends are not storable, and the representative investor must hold the market, so the model is closed by stipulating that the representative agent's consumption equals the sum of the two dividends: $C_t = D_{1t} + D_{2t}$.

2 The two-asset case

2.1 A simple example

Consider the problem of pricing the claim to asset 1's output in the simplest case $\gamma = 1$: log utility. We have

$$\begin{aligned} P_1 &= \mathbb{E}\int_0^\infty e^{-\rho t}\left(\frac{C_t}{C_0}\right)^{-1} \cdot D_{1t}\,dt \\ &= \mathbb{E}\int_0^\infty e^{-\rho t}\frac{D_{10}+D_{20}}{D_{1t}+D_{2t}} \cdot D_{1t}\,dt \\ &= (D_{10}+D_{20})\int_0^\infty e^{-\rho t}\mathbb{E}\left(\frac{1}{1+D_{2t}/D_{1t}}\right)\,dt \,, \end{aligned}$$

and unfortunately this expectation is not easy to calculate. If, say, the D_{it} are geometric Brownian motions, then we have to compute the expected value of the reciprocal of one plus a lognormal random variable. This, essentially, is the major analytical challenge confronted by Cochrane, Longstaff and Santa-Clara (2008).

Here, though, is an instructive case in which the expectation simplifies considerably. Suppose that $D_{2t} < D_{1t}$ at all times t. Perhaps, for example, D_{1t} is constant and initially larger than D_{2t}, which is subject to downward jumps at random times.[5] (The jumps may be random in size, but they must always be downwards.) Then $D_{2t}/D_{1t} < 1$ and so we can expand the expectation as a geometric sum. To make things simple, set $D_{1t} \equiv 1$: then,

$$\begin{aligned} \mathbb{E}\left(\frac{1}{1+D_{2t}}\right) &= \mathbb{E}\left[1 - D_{2t} + D_{2t}^2 - \dots\right] \\ &= \sum_{n=0}^{\infty}(-1)^n D_{20}^n \mathbb{E}\left[(D_{2t}/D_{20})^n\right] \\ &= \sum_{n=0}^{\infty}(-1)^n D_{20}^n e^{\boldsymbol{c}(0,n)t}. \end{aligned}$$

Substituting back, we find that

$$\begin{aligned} P_1 &= (1+D_{20}) \int_{t=0}^{\infty} e^{-\rho t} \sum_{n=0}^{\infty}(-1)^n D_{20}^n e^{\boldsymbol{c}(0,n)t}\, dt \\ &= (1+D_{20}) \sum_{n=0}^{\infty}(-1)^n D_{20}^n \int_{t=0}^{\infty} e^{-[\rho-\boldsymbol{c}(0,n)]t}\, dt \\ &= (1+D_{20}) \sum_{n=0}^{\infty} \frac{(-1)^n D_{20}^n}{\rho - \boldsymbol{c}(0,n)} \end{aligned}$$

If we define $s \equiv D_{10}/(D_{10}+D_{20})$ to be the share of asset 1 in global output—a definition which is maintained throughout—we can rewrite this in a form that is more directly comparable with subsequent results:

$$P/D_1 = \frac{1}{\sqrt{s(1-s)}} \sum_{n=0}^{\infty} \frac{(-1)^n \left(\frac{1-s}{s}\right)^{n+1/2}}{\rho - \boldsymbol{c}(0,n)}$$

P/D_1 is the price-dividend ratio of asset 1 at time 0. When time subscripts are dropped, here and elsewhere, the relevant time is time 0.

[5] This approach fails in the Brownian motion case, since if either D_{1t} or D_{2t} has a Brownian component we cannot say that $D_{2t} < D_{1t}$ with probability one.

This expression is not in closed form, but it is easy to evaluate numerically, once the process driving the dividends of asset 2—and hence $\boldsymbol{c}(0,n)$—is specified. For example, if asset 2's log dividend is subject to downward jumps of constant size $-b$ which occur at intervals dictated by a Poisson process with arrival rate ω, then $\boldsymbol{c}(0,n) = \omega(e^{-bn} - 1)$, so $\rho - \boldsymbol{c}(0,n) \to \rho + \omega$ as $n \to \infty$. Meanwhile, $(1-s)/s < 1$ so the terms in the numerator of the summand decline at geometric rate and numerical summation will converge fast.

The extremely special structure of this example made it legitimate to write $1/(1+D_{2t})$ as a geometric sum. In the general case, it will turn out to be possible to make an analogous move, writing the equivalent of $1/(1+D_{2t})$ as a Fourier integral before computing the expectation.

2.2 General solution

It is convenient to work with a generic asset with dividend stream $D_{\boldsymbol{\alpha},t} \equiv D_{1t}^{\alpha_1} D_{2t}^{\alpha_2}$, where $\boldsymbol{\alpha} \equiv (\alpha_1, \alpha_2) \in \{(1,0), (0,1), (0,0)\}$. The three alternatives represent asset 1, asset 2, and a riskless perpetuity respectively.

2.2.1 Prices

Asset prices turn out to depend on the value of a single state variable $s \in [0,1]$, the share of aggregate consumption contributed by the dividend of asset 1:

$$s = \frac{D_{10}}{D_{10} + D_{20}}.$$

It is often more convenient to work with the state variable u, a monotonic transformation of s which is defined by

$$u = \log\left(\frac{1-s}{s}\right) = y_{20} - y_{10}.$$

While s ranges between 0 and 1, u takes values between $-\infty$ and $+\infty$. As asset 1 becomes small, u tends to infinity; as asset 1 becomes large, u tends to minus infinity.

The following Proposition supplies an integral formula for the price-dividend ratio on the $\boldsymbol{\alpha}$-asset. The formula is perfectly suited for numerical implementation but also permits further analytical results to be derived.[6]

[6] i is the complex number $\sqrt{-1}$.

Proposition 1 (The pricing formula)**.** *The price-dividend ratio on an asset which pays dividend stream* $D_{\boldsymbol{\alpha},t} \equiv D_{1t}^{\alpha_1} D_{2t}^{\alpha_2}$ *is*

$$\frac{P_{\boldsymbol{\alpha}}}{D_{\boldsymbol{\alpha}}}(s) = \frac{1}{\sqrt{s^\gamma (1-s)^\gamma}} \int_{-\infty}^{\infty} \frac{\mathscr{F}_\gamma(v)\left(\frac{1-s}{s}\right)^{iv}}{\rho - \boldsymbol{c}(\alpha_1 - \gamma/2 - iv, \alpha_2 - \gamma/2 + iv)}\, dv\,, \tag{4}$$

where $\mathscr{F}_\gamma(v)$ *is defined by*

$$\mathscr{F}_\gamma(v) \equiv \frac{1}{2\pi} \cdot \frac{\Gamma(\gamma/2 + iv)\Gamma(\gamma/2 - iv)}{\Gamma(\gamma)}\,. \tag{5}$$

In terms of the state variable u*, this becomes*

$$\frac{P_{\boldsymbol{\alpha}}}{D_{\boldsymbol{\alpha}}}(u) = [2\cosh(u/2)]^\gamma \cdot \int_{-\infty}^{\infty} \frac{e^{iuv}\mathscr{F}_\gamma(v)}{\rho - \boldsymbol{c}(\alpha_1 - \gamma/2 - iv, \alpha_2 - \gamma/2 + iv)}\, dv\,. \tag{6}$$

Proof. The price of the $\boldsymbol{\alpha}$-asset is

$$\begin{aligned} P_{\boldsymbol{\alpha}} &= \mathbb{E}\int_0^\infty e^{-\rho t}\left(\frac{C_t}{C_0}\right)^{-\gamma} D_{1t}^{\alpha_1} D_{2t}^{\alpha_2}\, dt \\ &= (C_0)^\gamma \int_0^\infty e^{-\rho t}\, \mathbb{E}\left(\frac{e^{\alpha_1(y_{10}+\widetilde{y}_{1t})+\alpha_2(y_{20}+\widetilde{y}_{2t})}}{\left[e^{y_{10}+\widetilde{y}_{1t}} + e^{y_{20}+\widetilde{y}_{2t}}\right]^\gamma}\right) dt\,. \end{aligned}$$

It follows that

$$\frac{P_{\boldsymbol{\alpha}}}{D_{\boldsymbol{\alpha}}} = (e^{y_{10}} + e^{y_{20}})^\gamma \int_{t=0}^\infty e^{-\rho t}\, \mathbb{E}\left(\frac{e^{\alpha_1 \widetilde{y}_{1t} + \alpha_2 \widetilde{y}_{2t}}}{\left[e^{y_{10}+\widetilde{y}_{1t}} + e^{y_{20}+\widetilde{y}_{2t}}\right]^\gamma}\right) dt\,.$$

The expectation inside the integral is calculated, via a Fourier transform, in Appendix A.1.1. Substituting in from equation (28) of the Appendix, interchanging the order of integration—since the integrand is absolutely integrable, this is a legitimate application of Fubini's theorem—and writing u for $y_{20} - y_{10}$, we obtain (6):

$$\begin{aligned} \frac{P_{\boldsymbol{\alpha}}}{D_{\boldsymbol{\alpha}}} &= [2\cosh(u/2)]^\gamma \int_{v=-\infty}^\infty \int_{t=0}^\infty e^{-\rho t} e^{\boldsymbol{c}(\alpha_1-\gamma/2-iv, \alpha_2-\gamma/2+iv)t} \cdot e^{iuv}\mathscr{F}_\gamma(v)\, dt\, dv \\ &\overset{(a)}{=} [2\cosh(u/2)]^\gamma \int_{v=-\infty}^\infty \frac{e^{iuv}\mathscr{F}_\gamma(v)}{\rho - \boldsymbol{c}(\alpha_1 - \gamma/2 - iv, \alpha_2 - \gamma/2 + iv)}\, dv \end{aligned}$$

where $\mathscr{F}_\gamma(v)$ is as in (5). For equality (a) to hold, I have assumed that

$$\rho - \mathrm{Re}[\boldsymbol{c}(\alpha_1 - \gamma/2 - iv, \alpha_2 - \gamma/2 + iv)] > 0 \quad \text{for all } v \in \mathbb{R}.$$

I show in Appendix B that this follows from the apparently weaker assumption that the inequality holds at $v = 0$: $\rho - \boldsymbol{c}(\alpha_1 - \gamma/2, \alpha_2 - \gamma/2) > 0$. I assume that this holds when $(\alpha_1, \alpha_2) = (1, 0)$, $(0, 1)$, or $(0, 0)$. See Table 1 below. Finally, (4) follows from (6) by substituting $u = \log[(1-s)/s]$. □

The gamma function $\Gamma(z)$ that appears in (5) is defined for complex numbers z with positive real part by

$$\Gamma(z) = \int_0^\infty t^{z-1} e^{-t} \, dt \, .$$

For real v and integer $\gamma > 0$, $\mathscr{F}_\gamma(v)$ is a strictly positive function which is symmetric about $v = 0$, where it attains its maximum, and decays exponentially fast towards zero as v tends to plus or minus infinity.

In its present form, the pricing formula (4) appears rather complicated, but it is worth emphasizing that it allows for the stochastic process governing log outputs to be *any* Lévy process that leads to finite asset prices—a class which includes, for example, constant deterministic growth, drifting Brownian motion, compound Poisson processes, variance gamma processes, Normal inverse Gaussian processes, and a host of others, including linear combinations of the processes mentioned.

The proof of Proposition 1 showed that finiteness of the prices of the two assets—which implies that expected utility is finite—is assured by the assumptions that

$$\rho - \boldsymbol{c}(1-\gamma/2, -\gamma/2) > 0 \qquad \text{and} \qquad \rho - \boldsymbol{c}(-\gamma/2, 1-\gamma/2) > 0 \, . \tag{7}$$

I also make an assumption that ensures that perpetuities have finite prices:

$$\rho - \boldsymbol{c}(-\gamma/2, -\gamma/2) > 0 \, . \tag{8}$$

This restriction is not necessary from a mathematical point of view; I impose it because it seems empirically plausible that real perpetuities in zero net supply have finite prices. (If either of the assets in positive net supply *is* a perpetuity, then (8) is implied by (7).) After Proposition 3, I give an intuitive interpretation of these assumptions.

These assumptions ensure that aggregate wealth is finite for all $s \in (0,1)$. I also assume that aggregate wealth is finite at the one-tree limit points, $s = 0$ and $s = 1$. In the limit $s \to 1$, this requires that $\rho - \boldsymbol{c}(1-\gamma, 0) > 0$, and in the limit $s \to 0$, this requires that $\rho - \boldsymbol{c}(0, 1-\gamma) > 0$. These assumptions are summarized in Table 1.

For many practical purposes this is, in a sense, the end of the story, since the integral formula is very well behaved and can be calculated effectively instantly in *Mathematica* or *Maple*. After providing similar integral formulas for expected returns, the riskless rate, and bond yields, I take this simple and direct route in section 3. Nonetheless, it is possible to push the pen-and-paper approach further in the case in which log dividends follow drifting Brownian motions: the integral (4) is then soluble in closed form. See section 2.3.

Restriction	Reason
$\rho - \boldsymbol{c}(1-\gamma/2, -\gamma/2) > 0$	finite price of asset 1
$\rho - \boldsymbol{c}(-\gamma/2, 1-\gamma/2) > 0$	finite price of asset 2
$\rho - \boldsymbol{c}(-\gamma/2, -\gamma/2) > 0$	finite perpetuity price
$\rho - \boldsymbol{c}(1-\gamma, 0) > 0$	finite aggregate wealth in limit $s \to 1$
$\rho - \boldsymbol{c}(0, 1-\gamma) > 0$	finite aggregate wealth in limit $s \to 0$

Table 1: The restrictions imposed on the model.

2.2.2 Returns

An expression for the expected return on a general asset paying dividend stream $D_{\boldsymbol{\alpha},t}$ can be found in terms of integrals very similar to those that appear in the general price-dividend formula. The instantaneous expected return, $R_{\boldsymbol{\alpha}}$, is defined by

$$R_{\boldsymbol{\alpha}} dt \equiv \underbrace{\frac{\mathbb{E} dP_{\boldsymbol{\alpha}}}{P_{\boldsymbol{\alpha}}}}_{\text{capital gains}} + \underbrace{\frac{D_{\boldsymbol{\alpha}}}{P_{\boldsymbol{\alpha}}} dt}_{\text{dividend yield}} .$$

Proposition 2 (Expected returns)**.** *If γ is a positive integer, then $R_{\boldsymbol{\alpha}}$ is given by*

$$R_{\boldsymbol{\alpha}}(u) = \frac{\sum_{m=0}^{\gamma} \binom{\gamma}{m} e^{-mu} \int_{-\infty}^{\infty} h(v) e^{iuv} \cdot \boldsymbol{c}(\boldsymbol{w}_m(v))\, dv}{\sum_{m=0}^{\gamma} \binom{\gamma}{m} e^{-mu} \int_{-\infty}^{\infty} h(v) e^{iuv}\, dv} + \frac{D_{\boldsymbol{\alpha}}}{P_{\boldsymbol{\alpha}}}(u) . \tag{9}$$

where

$$h(v) \equiv \frac{\mathscr{F}_{\gamma}(v)}{\rho - \boldsymbol{c}(\alpha_1 - \gamma/2 - iv, \alpha_2 - \gamma/2 + iv)} ,$$

and

$$\boldsymbol{w}_m(v) \equiv (\alpha_1 - \gamma/2 + m - iv, \alpha_2 + \gamma/2 - m + iv) .$$

An analogous formula written in terms of the state variable s can be obtained by setting $u = \log[(1-s)/s]$ throughout (9)*.*

Proof. Appendix A contains the details of the capital gains calculation. The dividend yield component is given by the reciprocal of (6). □

2.2.3 Interest rates

Write B_T for the time-0 price of a zero-coupon bond which pays one unit of the consumption good at time T. The yield to time T, $\mathscr{Y}(T)$, is defined by $B_T = e^{-\mathscr{Y}(T)\cdot T}$. Interest rates are not constant unless the two assets have identical, perfectly correlated, output processes. For example, the prices of perpetuities and zero coupon bonds fluctuate over time. Define the instantaneous riskless rate as $r \equiv \lim_{T\downarrow 0} \mathscr{Y}(T)$.

The following Proposition summarizes the behavior of real interest rates, in terms of the state variable u. Depending on the stochastic process driving dividends, the model can generate upward- or downward-sloping curves and humped curves with a local maximum.

Proposition 3 (Real interest rates)**.** *The yield to time T is*

$$\mathscr{Y}(T) = \rho - \frac{1}{T}\log\left\{[2\cosh(u/2)]^{\gamma}\int_{-\infty}^{\infty}\mathscr{F}_{\gamma}(v)e^{iuv}\cdot e^{\boldsymbol{c}(-\gamma/2-iv,-\gamma/2+iv)T}\,dv\right\}. \tag{10}$$

The instantaneous riskless rate is

$$r = [2\cosh(u/2)]^{\gamma}\int_{-\infty}^{\infty}\mathscr{F}_{\gamma}(v)e^{iuv}\cdot[\rho - \boldsymbol{c}(-\gamma/2-iv,-\gamma/2+iv)]\,dv\,. \tag{11}$$

As before, we can set $u = \log[(1-s)/s]$ in (10) and (11) to express yields and the riskless rate in terms of the output share s.

The long rate is a constant, independent of the current state u, given by

$$\lim_{T\to\infty}\mathscr{Y}(T) = \rho - \boldsymbol{c}(-\gamma/2,-\gamma/2). \tag{12}$$

Proof. Expressions (10) and (11) (which follows by l'Hôpital's rule) are derived in Appendix A. Equation (12) follows from (10) by the method of steepest descent, after noting that the real part of $\boldsymbol{c}(-\gamma/2-iv,-\gamma/2+iv)$ achieves its maximum over $v\in\mathbb{R}$ when $v=0$, by the ridge property (see Appendix B). □

A perpetuity has finite price if $\rho - \boldsymbol{c}(-\gamma/2,-\gamma/2) > 0$. Equation (12) shows that this is equivalent to requiring that the long rate is strictly positive. Similarly, the conditions (7) that ensure finiteness of individual asset prices are equivalent to assumptions that the internal rates of return on the zero-coupon assets that pay D_{1T} and D_{2T} at time T are positive in the limit as $T\to\infty$.

2.3 The Brownian motion case

When dividends follow geometric Brownian motions[7] and risk aversion γ is an integer, closed-form solutions can be obtained for asset prices. Suppose, then, that log dividend processes are driven by a pair of Brownian motions, $dy_i = \mu_i\, dt + \sqrt{\sigma_{ii}}\, dz_i$, where dz_1 and dz_2 may be correlated: $\sqrt{\sigma_{11}\sigma_{22}}\, dz_1\, dz_2 = \sigma_{12}\, dt$.

The following result expresses the price-dividend ratio in terms of the hypergeometric function $F(a, b; c; z)$, which is defined for $|z| < 1$ by the power series

$$F(a,b;c;z) = 1 + \frac{a \cdot b}{1! \cdot c} z + \frac{a(a+1) \cdot b(b+1)}{2! \cdot c(c+1)} z^2 + \frac{a(a+1)(a+2) \cdot b(b+1)(b+2)}{3! \cdot c(c+1)(c+2)} z^3 + \cdots\,, \tag{13}$$

and for $|z| \geq 1$ by the integral representation

$$F(a,b;c;z) = \frac{\Gamma(c)}{\Gamma(b)\Gamma(c-b)} \int_0^1 w^{b-1}(1-w)^{c-b-1}(1-wz)^{-a}\, dw \quad \text{if Re } (c) > \text{Re } (b) > 0\,.$$

Proposition 4 (The Brownian motion case)**.** *When dividends follow geometric Brownian motions and γ is an integer, the price-dividend ratio of the $\boldsymbol{\alpha}$-asset is*

$$\begin{aligned} P/D_1(s) \quad &= \quad \frac{1}{B(\lambda_1 - \lambda_2)} \left[\frac{1}{(\gamma/2 + \lambda_1)\, s^\gamma}\; F\left(\gamma, \gamma/2 + \lambda_1; 1 + \gamma/2 + \lambda_1; \frac{s-1}{s}\right) + \right. \\ & \qquad \left. + \frac{1}{(\gamma/2 - \lambda_2)\,(1-s)^\gamma}\; F\left(\gamma, \gamma/2 - \lambda_2; 1 + \gamma/2 - \lambda_2; \frac{s}{s-1}\right) \right] \end{aligned} \tag{14}$$

The variables λ_1, λ_2, and B are given by

$$\begin{aligned} B &\equiv \frac{1}{2} X^2 \\ \lambda_1 &\equiv \frac{\sqrt{Y^2 + X^2 Z^2} - Y}{X^2} \\ \lambda_2 &\equiv -\frac{\sqrt{Y^2 + X^2 Z^2} + Y}{X^2}\,, \end{aligned}$$

where

$$\begin{aligned} X^2 &\equiv \sigma_{11} - 2\sigma_{12} + \sigma_{22} \\ Y &\equiv \mu_1 - \mu_2 + \alpha_1(\sigma_{11} - \sigma_{12}) - \alpha_2(\sigma_{22} - \sigma_{12}) - \frac{\gamma}{2}(\sigma_{11} - \sigma_{22}) \\ Z^2 &\equiv 2(\rho - \alpha_1\mu_1 - \alpha_2\mu_2) - (\alpha_1^2\sigma_{11} + 2\alpha_1\alpha_2\sigma_{12} + \alpha_2^2\sigma_{22}) + \\ & \quad + \gamma\left[\mu_1 + \mu_2 + \alpha_1\sigma_{11} + (\alpha_1 + \alpha_2)\sigma_{12} + \alpha_2\sigma_{22}\right] - \frac{\gamma^2}{4}(\sigma_{11} + 2\sigma_{12} + \sigma_{22}) \end{aligned}$$

[7] Under the Lévy process assumption, this is the unique case in which dividends are not subject to jumps. See Rogers and Williams (2000, pp. 76–77) for a proof.

and as the notation suggests, X^2 and Z^2 are strictly positive.

The instantaneous riskless rate is given by

$$\begin{aligned} r &= \rho + \gamma \left[s \left(\mu_1 + \frac{\sigma_{11}}{2} \right) + (1-s) \left(\mu_2 + \frac{\sigma_{22}}{2} \right) \right] - \\ &\quad - \frac{\gamma(\gamma+1)}{2} \left[s^2 \sigma_{11} + 2s(1-s)\sigma_{12} + (1-s)^2 \sigma_{22} \right] . \end{aligned} \tag{15}$$

Proof. In brief, the result follows by showing that the integral formula (6) is equal to the limit of a sequence of contour integrals around increasingly large semicircles in the upper half of the complex plane. By the residue theorem, this limit can be evaluated by summing all residues in the upper half-plane of the integrand in (6). The resulting limit is (14). Appendix C has the details. In the Brownian motion case, the riskless rate r is given by $r\,dt = -\mathbb{E}(dM/M)$, where $M_t \equiv e^{-\rho t} C_t^{-\gamma}$; (15) follows by Itô's lemma. □

Equation (14) generalizes the result of Cochrane, Longstaff and Santa-Clara (2008) (equation (50) in their paper) beyond the log utility special case. Since it is not obviously more informative than the more general (6), which applies equally well to non-Brownian dividend processes, I do not supply a formula for the expected return although, given the above result, it could be calculated along the same lines as the analogous calculation in Cochrane, Longstaff and Santa-Clara (2008).

3 Two calibrations

I now present two simple calibrations. In each, the representative agent has time discount rate $\rho = 0.03$ and relative risk aversion $\gamma = 4$.

3.1 Dividends follow geometric Brownian motions

To explore the distinctive features of the model in a setting that is as simple as possible, consider a calibration in which the two assets are independent and have dividends which follow geometric Brownian motions. Each has mean log dividend growth of 2% and dividend volatility of 10%. In the notation of equation (2), $\mu_1 = \mu_2 = 0.02$, $\sigma_{11} = \sigma_{22} = 0.1^2$, and $\sigma_{12} = 0$.

Although the dividend processes for the individual assets are i.i.d., consumption is *not* i.i.d., as documented in Figure 1. In this calibration, both assets have the same mean dividend growth, so mean consumption growth does not vary with s. But

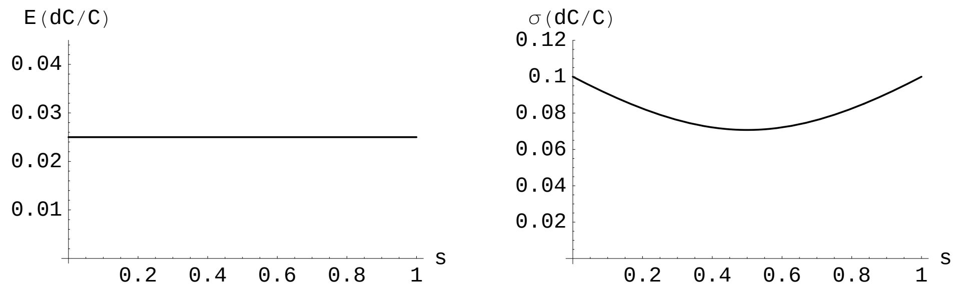

(a) $\mathbb{E}\left(\frac{dC}{C}\right)$ (b) $\sigma\left(\frac{dC}{C}\right)$

Figure 1: Left: Mean consumption growth, $\mathbb{E}(dC/C)$, against asset 1's dividend share, s. Right: The standard deviation of consumption growth, $\sigma(dC/C)$, against s.

the standard deviation of consumption growth does vary: it is lower "in the middle", where there is most diversification. At the edges, where s is close to 0 or to 1, one of the two assets dominates the economy, and consumption growth is more volatile: the representative agent's eggs are all in one technological basket.

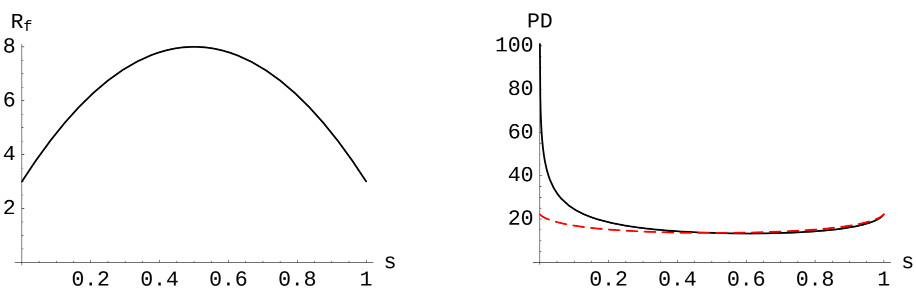

(a) Riskless rate (b) P/D

Figure 2: Left: The riskless rate against s. Right: The price-dividend ratio of asset 1 (solid) and of the market (dashed) against s.

Time-varying consumption growth volatility leads to a time-varying riskless rate. Figure 2a plots the riskless rate against asset 1's share of output s. Riskless rates are high for intermediate values of s because consumption volatility is low, which diminishes the motive for precautionary saving.

Figure 2b shows the price-dividend ratio of asset 1 and of the market. When s is small, asset 1 contributes a small proportion of consumption. It therefore has little systematic risk, and hence a high valuation. As its dividend share increases, its discount rate increases both because the riskless rate increases and because its risk premium increases, as discussed further below.

The model predicts that assets may have very high price-dividend ratios but not very low price-dividend ratios. Moreover, as an asset's share approaches zero, its price-dividend ratio becomes sensitively dependent on its share. This case is of particular interest because it represents a stark contrast to models in which price-dividend ratios are constant (as in the $N = 1$ case, for example); it is explored in section 4.

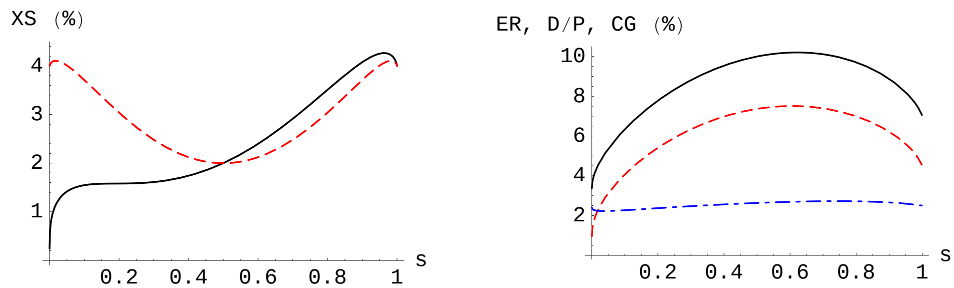

(a) Excess return on asset 1 (b) Expected return decomposition

Figure 3: Left: The excess return on asset 1 (solid) and on the market (dashed), against s. Right: Decomposition of expected returns (solid) into dividend yield (dashed) and expected capital gains (dot-dashed).

Figure 3a shows how the risk premium on asset 1 and on the market depends on the state variable s. Due to the diversification effect discussed above, the market risk premium is smallest when the two assets are of equal size. The risk premium on asset 1 increases as its dividend share increases. As s tends to zero, the risk premium on asset 1 tends to zero. The figure shows, however, that in this calibration even very small assets earn economically significant risk premia. In other calibrations, idiosyncratic assets can earn strictly positive risk premia even in the limit.

Figure 3b decomposes expected returns into dividend yield plus expected capital gain. In this calibration, almost all cross-sectional variation in expected returns can be attributed to cross-sectional differences in dividend yield.

Figure 4a plots expected returns and risk premia against dividend yield. There is a value-growth effect: an asset with a high valuation earns a low excess return.[8] Figure 4b demonstrates that the excess return on a zero-cost investment in a value-minus-growth portfolio is increasing in the value spread (that is, the difference in dividend yield between the value and the growth asset). This echoes the empirical finding

[8]This is a time-series statement: there are only two assets in the cross-section. Section 5 extends the analysis to N assets. Since dividend growth is i.i.d., high price-dividend ratios must, mechanically, forecast low expected returns in this case, too. See Cochrane (2005), p. 399.

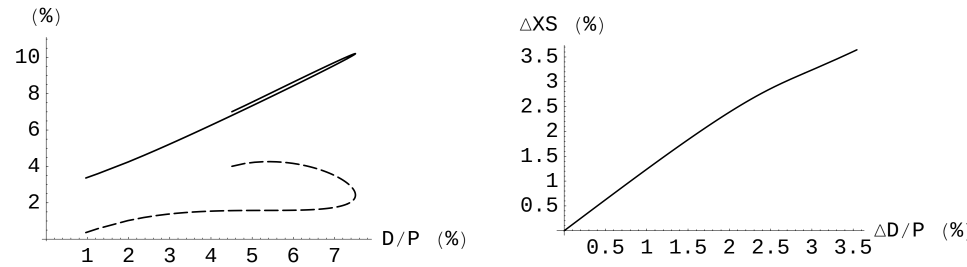

(a) Expected returns and expected excess returns on asset 1 against D/P.

(b) Expected excess returns on the value-minus-growth strategy, plotted against the value spread.

Figure 4: Left: Expected returns (solid) and expected excess returns (dashed) on asset 1 against its dividend yield. Right: Expected excess return on the value-minus-growth strategy against the value spread.

of Cohen, Polk and Vuolteenaho (2003) that "the expected return on value-minus-growth strategies is atypically high at times when their spread in book-to-market ratios is wide."

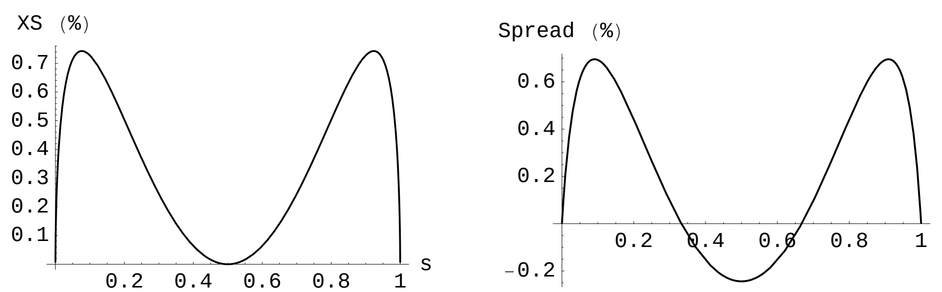

(a) Excess returns on a perpetuity.

(b) The yield spread.

Figure 5: A high yield spread, $\mathscr{Y}(30) - \mathscr{Y}(0)$, signals high expected excess returns on a perpetuity.

It is also of interest to consider the behavior of assets in zero net supply, such as perpetuities and zero coupon bonds. Figure 5a plots the risk premium on a real perpetuity which pays one unit of consumption good per unit time. Figure 5b shows how the spread in yields between a 30-year zero-coupon bond and the instantaneous riskless rate varies with s. A high yield spread forecasts high excess returns on long-term bonds. Looking back at figure 3a, we see that a high yield spread also forecasts high excess returns on the market.

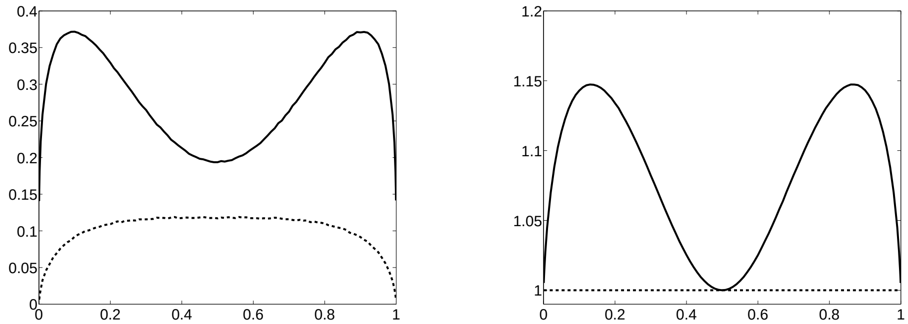

(a) Correlation between asset returns. (b) Excess volatility on the market.

Figure 6: Left: The correlation between the returns of asset 1 and asset 2 against s. Right: The ratio of market return volatility to dividend volatility against s. Solid lines, $\gamma = 4$; dashed lines, $\gamma = 1$.

Figure 6a demonstrates that the model generates significant comovement between the returns of the two assets, even though the two assets have independent fundamentals.[9] There is considerably more comovement when $\gamma = 4$ than in the log utility case (dashed line). Figure 6b shows that the model generates excess volatility in the aggregate market when $\gamma > 1$. (When $\gamma = 1$—the log utility case, indicated with a dashed line—there is no excess volatility because the price-dividend ratio of the aggregate market is constant. For the same reason, there is no excess volatility in the $\gamma = 4$ case when $s = 1/2$: the market price-dividend ratio is locally flat, as a function of s, at this point.)

What drives asset 1's returns? In the two-asset case, two types of shock move an asset's price: a shock to its dividends, or a shock to the other asset's dividends, which changes the asset's price by changing its price-dividend ratio. In the terminology of

[9] These figures, unlike the preceding ones, are calculated by Monte Carlo methods, as follows. For each of 109 different starting values of $s \in [0, 1]$, I generate 4000 sample paths of log dividends. (The 109 different values are the points 0.01, 0.02, ..., 0.99, five points between 0 and 0.01, and five points between 0.99 and 1.) Each sample path simulates a drifting Brownian motion over a very short time horizon: 3×10^{-5} years, slightly less than 16 minutes. Over this time horizon, each drifting Brownian motion is simulated by dividing the interval into 600 time steps; Normal random variables determine the evolution of log dividends between these time steps. Given a particular sample path for dividends, prices can be calculated, given the price-dividend functions; and hence also total returns, and the covariance matrix of realized returns on the two assets. Finally, I estimate variances and covariance between the two assets, at each value of s, by averaging over the covariance matrices estimated for each of the 4000 sample paths.

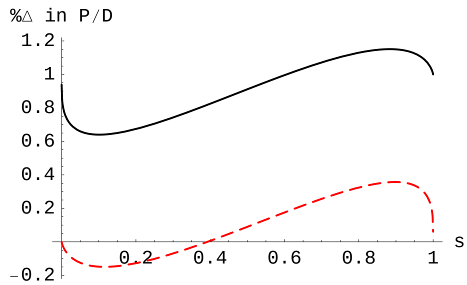

(a) Response to cashflow shock to asset 1.

Figure 7: The response of asset 1 (solid) and asset 2 (dashed) to a 1% increase in the dividend of asset 1.

Campbell (1991), the first type of shock corresponds to the arrival of "cashflow news" and the second to the arrival of "discount-rate news". Figure 7a plots the percentage price response of asset 1 (solid) and asset 2 (dashed) to a 1% increase in asset 1's dividends. When asset 1 is small, there is a momentum effect: it underreacts to good news about its own cashflow shock and asset 2 moves in the opposite direction. When asset 1 is large, it overreacts to good news about its own cashflow shock, and asset 2 moves in the same direction. Note also that asset 2's price moves considerably more, in response to dividend news for asset 1, when asset 1 is large than when asset 1 is small. I explore these cross-asset dynamics further in Section 5.2, where I present a more realistic calibration.

3.2 Dividends are subject to occasional disasters

The second calibration is intended to highlight the effect of disasters. Again, the two assets are symmetric for simplicity. In the notation of equation (2), the drifts are $\mu_1 = \mu_2 = 0.02$. The two Brownian motions driving dividends are independent and each has volatility of 2%, so $\sigma_{11} = \sigma_{22} = 0.02^2$ and $\sigma_{12} = 0$.

There are also jumps in dividends, caused by the arrival of disasters, of which there are three types. One type affects only asset 1: it arrives at times dictated by a Poisson process with rate 0.017/2. When the disaster strikes, it shocks log dividends by a Normal random variable with mean -0.38 and standard deviation 0.25. The second is exactly the same, except that it affects only asset 2. The third type arrives at rate 0.017/2 and shocks the log dividends of *both* assets by the same amount,[10] which is, again, a random variable with mean −0.38 and standard deviation of 0.25. If the two assets are thought of as claims to a country's output, then the first two types are examples of local disasters while the third is a global disaster. From the perspective of either asset, then, disasters occur at rate $0.017/2 + 0.017/2 = 0.017$: on average, about once every 60 years. There is a 50-50 chance that any given disaster is local or global. These disaster arrival rates—and the mean and standard deviation of the disaster sizes—are chosen to match exactly the empirical disaster frequency estimated by Barro (2006), and to match approximately the disaster size distribution documented in the same paper. Taking everything into account, these values imply an unconditional mean dividend growth rate (in levels, not logs) of 1.6%. Conditional on disasters not occurring, the mean dividend growth rate is 2.0%.

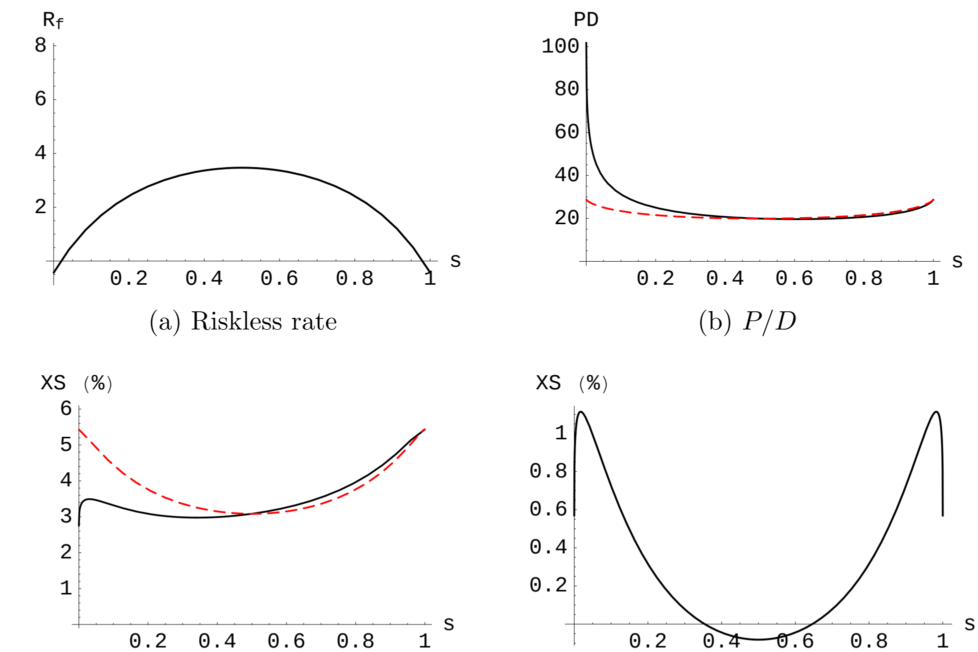

(a) Riskless rate

(b) P/D

(c) Excess returns on asset 1 and the market

(d) Excess returns on a perpetuity

Figure 8: The riskless rate; price-dividend ratio on asset 1 (solid) and on the market (dashed); excess returns on asset 1 (solid) and on the market (dashed); and excess returns on a perpetuity.

[10]These disasters are therefore simultaneous and of perfectly correlated—in fact, identical—sizes; the framework also easily handles the case in which disasters are simultaneous but uncorrelated or imperfectly correlated.

Figure 8 exhibits the central features of asset prices and returns in this calibration. In broad outline, the pictures are similar to those presented previously—and for the same reasons—but some new features stand out. The riskless rate is lower across the range of values of s. Also, despite considerably lower Brownian volatility, the presence of jumps induces a higher risk premium, both at the individual asset level and at the market level. As in Rietz (1988) and Barro (2006), incorporating rare disasters makes it easier to match the observed riskless rate and equity premium. Figure 8c shows that an asset's excess return can decline even as its share (and hence correlation with overall consumption) increases, if the aggregate risk premium declines suffciently quickly. Duffee (2005) argues that this is a feature of the data. A feature distinctive to jumps is that disasters can propagate to apparently safe assets: since the state variable can jump, interest rates can jump, and hence bond prices can jump. Consequently, when the current riskless rate is low (for s close to 0 or 1), the risk premium on a perpetuity is significantly higher than previously, despite the fact that disasters do not affect its cashflows. A perpetuity earns a negative risk premium near $s = 1/2$, since long-dated bonds then act as a hedge against disasters: when a disaster strikes one of the assets, interest rates drop and the price of a long-dated bond jumps up.

To emphasize how disasters propagate across assets, Figure 9 plots a single sample time series. Time, along the x-axis, runs from 0 to 60 years. The sequence of figures should be read clockwise, starting from the top left. Asset 1 (in red) is the small asset, with an initial dividend share of 10%. Asset 2 is shown in black. From exogenous dividend processes we calculate the dividend share of asset 1, and hence price-dividend ratios. Finally, from dividends and price-dividend ratios, we calculate prices.

In the particular realization shown here, each asset suffers one negative shock to fundamentals; there is no "global" shock. When the large asset suffers its disaster, after about 26 years, its dividend drops by 25% and its price drops by 28%. Two forces act on the small asset. A disaster to the large asset makes the economy more balanced, so riskless rates jump up; at the same time, the risk premium on the small asset jumps up because it is a larger part of the economy. These effects act in the same direction, and the small asset experiences a downward price jump of 8.2%: contagion.

When the small asset suffers its disaster, after about 49 years, its dividend drops by 39% and its price drops by 30%. Now, two *opposing* forces act on the large asset. On one hand, its risk premium rises as it is a larger share of the market. On the other, the riskless rate declines in response to the increasingly unbalanced world.

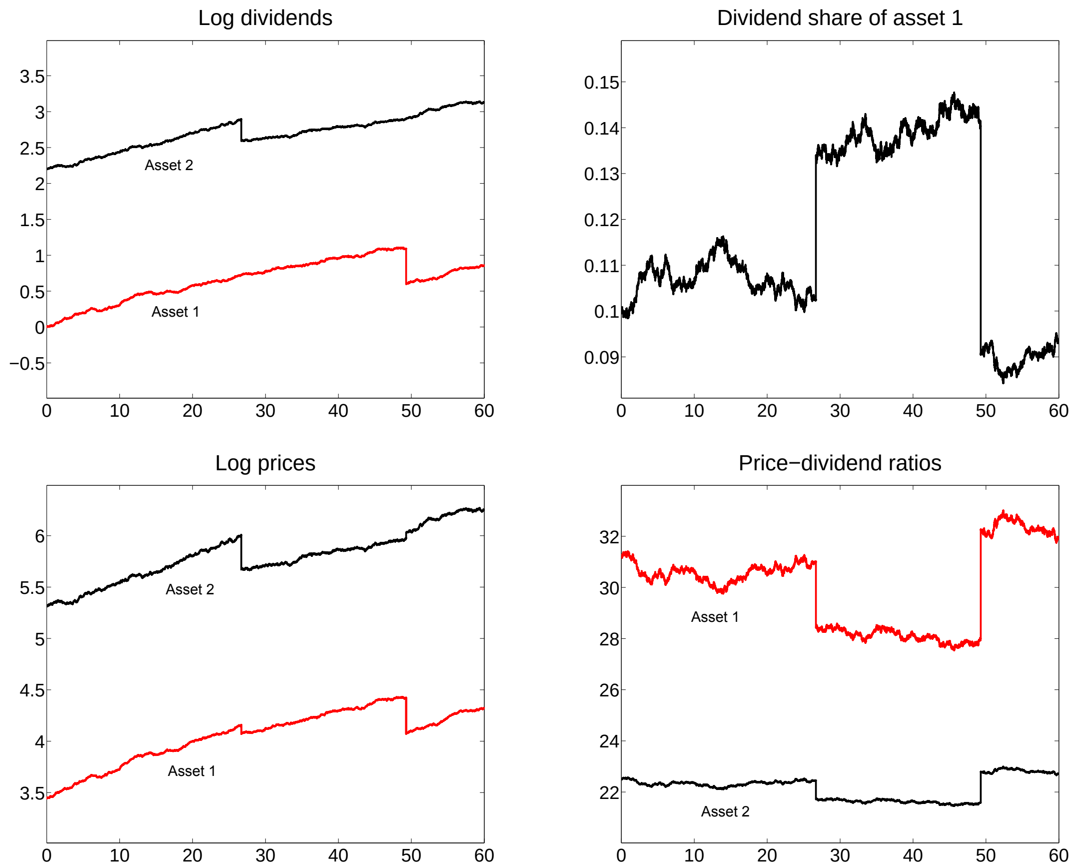

Figure 9: Dividends, dividend share, prices, and price-dividend ratios against time.

The riskless rate effect dominates, and the large asset experiences an upward price jump of 5.7%: flight-to-quality.

We can also calculate rolling 1-year realized return correlations along this sample path, as shown in Figure 10. During normal times, the correlation hovers around 0.3, despite the fact that, conditional on no jumps, the two assets have independent dividend streams. When the first disaster ("contagion") takes place, the measured correlation spikes up almost as far as $+1$ due to the spectacular outlying return. When the second disaster ("flight-to-quality") takes place, the measured correlation spikes down almost as far as -1. Despite the fact that naively calculated correlations display occasional spikes, the correlation between the two assets, conditional on some given s, is constant over time—and is economically significant even if one conditions on jumps not taking place. These results are therefore reminiscent of the findings of Forbes and Rigobon (2002), who demonstrate that although naively calculated correlations

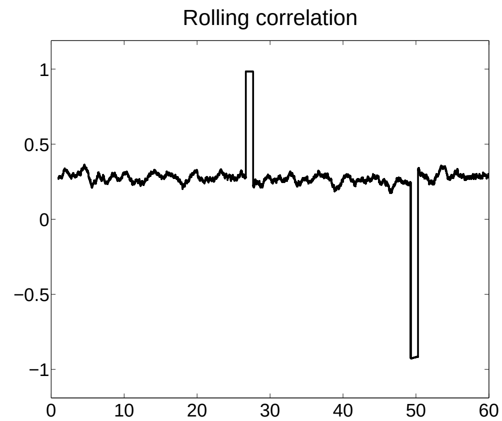

Figure 10: The one-year rolling correlation between assets 1 and 2, calculated along the sample path of Figure 9.

spike at times of crisis, once one corrects for the heteroskedasticity induced by high market volatility at times of crisis, it can be seen that markets have a high level of "interdependence" in all states of the world.

4 Equilibrium pricing of small assets

A distinctive qualitative prediction of the model is that there should exist extreme growth assets, but not extreme value assets. (Look back at the left-hand side of Figure 2b.) The extreme growth case also represents the starkest departure from simple models in which price-dividend ratios are constant (as, for example, in a one-tree model with power utility and i.i.d. dividend growth). Furthermore, it is important to understand whether the complicated dynamics exhibited above are relevant for small assets. These considerations lead me to investigate the price behavior of asset 1 in the limit $s \to 0$ in which it becomes tiny relative to the rest of the market.

To preview the results, consider the problem of pricing a negligibly small asset, whose fundamentals are independent of all other assets, in an environment in which the (real) riskless rate is 6%. If the small asset has mean dividend growth rate of 4%, the following logic seems plausible. Since the asset is negligibly small, it need not earn a risk premium, so the appropriate discount rate is the riskless rate. Next, since dividends are i.i.d., it seems sensible to apply the Gordon growth model to conclude that for this small asset, dividend yield = riskless rate − mean dividend growth =

2%. It turns out that this argument can be made formal; I do so below.

Now, consider the empirically more relevant situation in which the riskless real rate is 2%. If the asset does not earn a risk premium, Gordon growth logic seems to suggest that the dividend yield should be $2\% - 4\% = -2\%$, an obviously nonsensical result.

To investigate this issue, I now return to the general setup in which dividends may be correlated, subject to jumps, and so on, and make a pair of definitions.

Definition 2. *If the inequality*

$$\rho - \boldsymbol{c}(1, -\gamma) > 0 \tag{16}$$

holds then we are in the subcritical *case.*

If the reverse inequality

$$\rho - \boldsymbol{c}(1, -\gamma) < 0 \tag{17}$$

holds then we are in the supercritical *case.*[11]

Define z^* to be the unique $z > \gamma/2 - 1$ that satisfies

$$\rho - \boldsymbol{c}(1 - \gamma/2 + z, -\gamma/2 - z) = 0. \tag{18}$$

(If there is no such z^*, let $z^* = \infty$.)

In the supercritical case we have $z^* \in (\gamma/2 - 1, \gamma/2)$ because the left-hand side of (18) is positive at $z = \gamma/2 - 1$ by the finiteness assumption in Table 1 and negative at $z = \gamma/2$ by (17); similarly, in the subcritical case, $z^* > \gamma/2$. If dividends follow geometric Brownian motions, for example, then (18) is simply a quadratic equation in z. More generally, the fact that the solution is unique follows from the fact, proved in Appendix D, that $\rho - \boldsymbol{c}(1 - \gamma/2 + z, -\gamma/2 - z)$ is a concave function of z.

The next two Propositions supply various asymptotics. Bars above variables indicate limits as $s \to 0$, so for example $\overline{R_f} = \lim_{s\to 0} R_f(s)$. To highlight the link with the traditional Gordon growth formula, I write $G_1 \equiv \boldsymbol{c}(1, 0)$ and $G_2 \equiv \boldsymbol{c}(0, 1)$ for (log) mean dividend growth on assets 1 and 2 respectively, and $\overline{R_1}$ and $\overline{R_2}$ for the

[11] There is also the *critical* case in which $\rho - \boldsymbol{c}(1, -\gamma) = 0$ and $z^* = \gamma/2$; I omit it for the sake of brevity. Briefly, price-dividend ratios are asymptotically infinite and excess returns asymptotically zero, assuming independent dividend growth. The simple example presented in Section 1 of Cochrane, Longstaff and Santa-Clara (2008) is precisely critical. This is no coincidence: the condition that implies criticality also ensures that the expression for the price-dividend ratio is relatively simple. Details are available from the author.

limiting expected instantaneous returns on assets 1 and 2. Finally, I write $\overline{XS_1}$ for the limiting excess return on asset 1.

Proposition 5. *In the subcritical case, we have*

$$\begin{aligned}\overline{R_f} &= \rho - \boldsymbol{c}(0,-\gamma)\\ \overline{D/P_1} &= \rho - \boldsymbol{c}(1,-\gamma)\\ \overline{XS_1} &= \boldsymbol{c}(1,0) + \boldsymbol{c}(0,-\gamma) - \boldsymbol{c}(1,-\gamma)\end{aligned}$$

The Gordon growth model holds for a small asset: $\overline{D/P_1} = \overline{R_1} - \overline{G_1}$.
If the two assets are independent, then $0 = \overline{XS_1} < \overline{XS_2}$.

Proof. See Appendix D. □

The results of Proposition 5 correspond to the first example above. A small idiosyncratic asset with i.i.d. dividend growth earns no risk premium, and can be valued with the Gordon growth model. In the supercritical case, though, more intriguing behavior emerges.

Proposition 6. *In the supercritical case, we have*

$$\begin{aligned}\overline{R_f} &= \rho - \boldsymbol{c}(0,-\gamma)\\ \overline{D/P_1} &= 0\\ \overline{XS_1} &= \boldsymbol{c}(1-\gamma/2+z^*,\gamma/2-z^*) + \boldsymbol{c}(0,-\gamma) - \boldsymbol{c}(1-\gamma/2+z^*,-\gamma/2-z^*)\end{aligned}$$

If the two assets are independent, then $0 < \overline{XS_1} < \overline{XS_2}$. *If* $G_1 \geq G_2$, *then* $\overline{D/P_1} > \overline{R_1} - G_1$, *whether or not the assets are independent.*

Proof. See Appendix D. □

To understand what is going on, consider the case in which dividend growth is independent across assets, so that the risk in question is both small and idiosyncratic. Proposition 6 demonstrates that in the supercritical regime, such an asset has an enormous valuation ratio—reminiscent of Pástor and Veronesi (2003, 2006)—and earns a strictly positive risk premium. Since the enormous valuation implies that the asset's dividend yield is zero in the limit, the expected return on the asset is entirely due to expected capital gains.

At first sight, the implication in Proposition 6 that the price-dividend ratio of the small asset is infinite in the limit is unsettling. But note that this does not imply that the price-consumption ratio of the small asset is infinite, since

$$\frac{P_1}{C} = \frac{D_1}{D_1 + D_2} \cdot \frac{P_1}{D_1} = s \cdot \frac{P_1}{D_1},$$

so if P_1/D_1 tends to infinity more slowly than s tends to zero, the price-consumption ratio goes to zero in the limit. I show in Appendix D that this is ensured by the maintained assumption that $\rho - \boldsymbol{c}(0, 1-\gamma) > 0$.

Examination of conditions (16) and (17) reveals that the supercritical regime occurs whenever ρ is small, γ is large, or there is significant risk in the economy (represented by high curvature of the CGF).

4.1 Time-series properties near the small-asset limit

When $z^* < \gamma/2$, the previous section showed that surprising features emerge in the small asset limit. I now consider the case $z^* > \gamma/2$ in more detail. This case is not so extreme, because price-dividend ratios are finite in the limit, and it is possible to find simple closed-form approximations of the integral formulas to leading order in s. These closed forms characterize behavior not only *at* the limit point $s \downarrow 0$ but also *near* the limit point, and it turns out that there is a striking linear relationship between price-dividend ratios and expected excess returns.

The riskless rate, for example, is approximately linear in s for s close to zero:

$$R_f \doteq A + B \cdot s,$$

where the notation $a \doteq b$ means "a equals b plus higher-order terms in s", and A and B are constants. A equals $\overline{R_f}$, given in Proposition 5. The value of B is provided in the Appendix; it is determined by preference parameters, ρ and γ, and the technological environment, $\boldsymbol{c}(\cdot, \cdot)$.

When $z^* > \gamma/2 + 1$, the price-dividend ratio and excess return on the small asset are also affine functions of s. The dynamics are more interesting when $\gamma/2 < z^* < \gamma/2 + 1$, so in what follows, I restrict attention to this case.

Proposition 7. *When $\gamma/2 < z^* < \gamma/2 + 1$, the price-dividend ratio on the small asset and its excess return are given, to leading order in s, by*

$$\begin{aligned} P/D_1 &\doteq C - D \cdot s^{z^* - \gamma/2} \\ XS_1 &\doteq E + F \cdot s^{z^* - \gamma/2} \end{aligned}$$

where $C > 0$, $D > 0$, E and F are constants given in the appendix. If the assets have independent fundamentals, then $E = 0$ and $F > 0$.

So the riskless rate is an affine function of s, while the dividend yield and excess return is affine in $s^{z^*-\gamma/2}$. The significant feature of this expression is that $z^* - \gamma/2 \in (0,1)$, so $s^{z^*-\gamma/2}$ is very much larger in magnitude than s when $s \approx 0$: its derivative with respect to s is infinite at zero. Therefore, changes in price-dividend ratio (which we already knew would be associated with changes in expected returns, since dividend growth is unforecastable) can in fact be attributed more precisely to changes in expected *excess* returns.

Proposition 8. *In the time series, there is a simple linear relationship between the price-dividend ratio of the small asset and its expected excess return:*

$$P/D_1 \doteq G - H \cdot XS_1. \tag{19}$$

If the assets have independent fundamentals, then $H > 0$.

Proof. Follows immediately from the previous result by substituting out $s^{z^*-\gamma/2}$, with $G = C + DE/F$ and $H = D/F$. □

Since variation in the riskless rate is negligible by comparison with variation in expected excess returns and in P/D, we could also substitute expected return in place of expected excess return in (19), using the constant to absorb extra terms; but the point is that in equilibrium, the variation comes from movements in expected *excess* returns, not from movements in the riskless rate.

4.2 An example

I now exhibit these phenomena in the simple Brownian motion example considered earlier. This will make it clear that, first, the supercritical case is neither pathological nor dependent on extreme parameter values and, second, the size of the excess return effects documented above is economically meaningful. To recap, the world is symmetric, and the two assets are independent with 2% mean dividend growth and 10% dividend volatility.

As usual, $\gamma = 4$. If $\rho = 0.05$, then $\gamma/2 < z^* \approx 2.46 < \gamma/2 + 1$, so we are in the subcritical case analyzed in Propositions 5, 7, and 8.[12] If on the other hand $\rho = 0.01$, then $z^* \approx 1.68 < \gamma/2$, so we are in the supercritical case of Proposition 6.

[12]In the earlier calibrations, I set $\rho = 0.03$. This case is also subcritical with $z^* \in (\gamma/2, \gamma/2 + 1)$. I use $\rho = 0.05$ here to make the distinction between the two cases clearer in the figures.

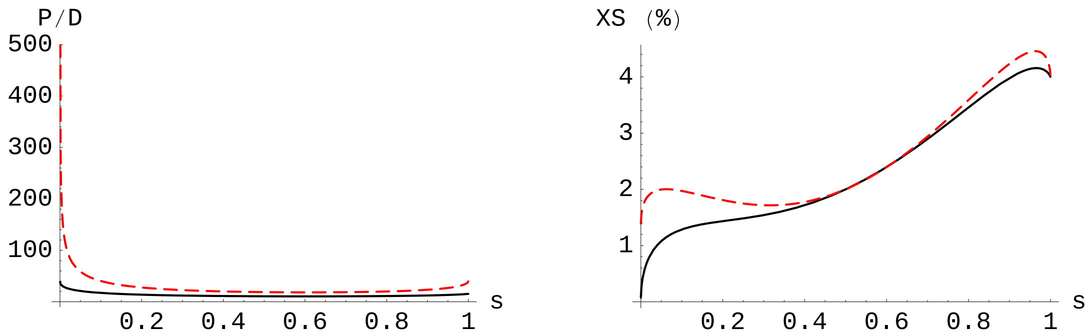

(a) Asset 1's price-dividend ratio (b) Asset 1's excess return

Figure 11: Left: Price-dividend ratio of asset 1 against s. Right: Excess return of asset 1 against s. Supercritical case is dashed, subcritical case is solid.

Figure 11 shows the price-dividend ratio and excess return of asset 1 against s. The asymptotic limits are to the left of the graph, as $s \downarrow 0$. In the subcritical case, the price-dividend ratio remains below 40 for all s and the excess return tends to zero. In the supercritical case, the price-dividend ratio explodes and the excess return tends to roughly 1.3 per cent. (Notice also that for intermediate values of the state variable, the risk premium on asset 1 is not sensitive to the value of ρ, as would be the case in a standard one-tree model.) Asymptotically, the dividend yield is zero, so the expected return on the small asset can be entirely attributed to expected capital gains.

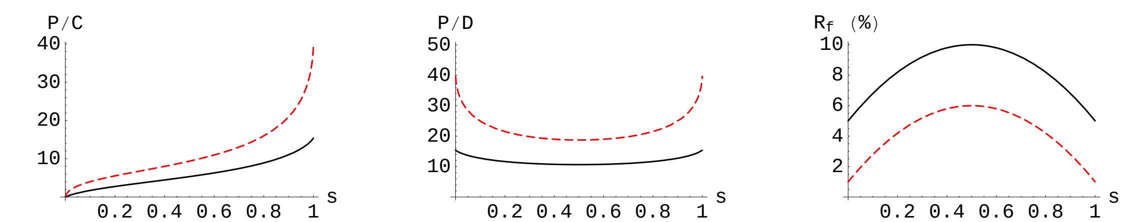

(a) Asset 1's price-consumption ratio (b) Market price-dividend ratio (c) Riskless rate

Figure 12: The price-consumption ratio of asset 1, market price-dividend ratio and riskless rate plotted against asset 1's share of output, s. Supercritical, dashed; subcritical, solid.

Finally, to allay suspicions that something strange is going on in the background, Figure 12 demonstrates that asset 1's price-consumption ratio, the market price-dividend ratio and the riskless rate are all well-behaved in the limit.

5 N assets

The results of Section 2.2 can be generalized to the case in which consumption is provided by the output of N assets, $C_t = D_{1t} + D_{2t} + \cdots + D_{Nt}$.

With this modification, equations (1)–(3) are unchanged, except that boldface vectors are now understood to have N entries, as opposed to just two. The fundamental ideas underlying the calculation are also the same. The main technical difficulty lies in calculating $\mathscr{F}_\gamma^N(\boldsymbol{v}) \equiv \mathscr{F}_\gamma^N(v_1, \ldots, v_{N-1})$, the generalization of $\mathscr{F}_\gamma(v)$ to the N-tree case. It turns out that we have

$$\mathscr{F}_\gamma^N(\boldsymbol{v}) = \frac{\Gamma\left(\gamma/N + iv_1 + iv_2 + \ldots + iv_{N-1}\right)}{(2\pi)^{N-1}\Gamma(\gamma)} \cdot \prod_{k=1}^{N-1} \Gamma\left(\gamma/N - iv_k\right). \tag{20}$$

Before stating the main result, it will be useful to recall some old, and to define some new, notation. Let $\boldsymbol{e}_j$ be an N-vector with a one at the jth entry and zeros elsewhere, and define the N-vectors $\boldsymbol{y}_0 \equiv (y_{10}, \ldots, y_{N0})'$ and $\boldsymbol{\gamma} \equiv (\gamma, \ldots, \gamma)'$, and the $(N-1) \times N$ matrix $\boldsymbol{U}$ and the $(N-1)$-vector $\boldsymbol{u}$ by

$$\boldsymbol{U} \equiv \begin{pmatrix} -1 & 1 & 0 & \cdots & 0 \\ -1 & 0 & 1 & \ddots & \vdots \\ \vdots & \vdots & \ddots & \ddots & 0 \\ -1 & 0 & \cdots & 0 & 1 \end{pmatrix} \quad \text{and} \quad \boldsymbol{u} \equiv \begin{pmatrix} u_2 \\ u_3 \\ \vdots \\ u_N \end{pmatrix} \equiv \boldsymbol{U}\boldsymbol{y}_0 . \tag{21}$$

In the two-asset case, there was one state variable. We worked with s, the dividend share of asset one, or with $u = \log(1-s)/s = y_{20} - y_{10}$. With N assets, there are $N-1$ state variables. One natural set of state variables is $\{s_i\}$, $i = 1, \ldots, N-1$, where

$$s_i = \frac{D_{i0}}{D_{10} + \cdots + D_{N0}}$$

is the dividend share of asset i; in fact, though, it turns out to be more convenient to work with the $(N-1)$-dimensional state vector $\boldsymbol{u}$. The first entry of $\boldsymbol{u}$ is $u_2 = y_{20} - y_{10}$, which corresponds to the state variable u of previous sections. More generally, $u_k = y_{k0} - y_{10}$ is a measure of the size of asset k relative to asset 1. Consistent with this notation, I will also write $u_1 \equiv y_{10} - y_{10} = 0$ and define the N-vector $\boldsymbol{u}_+ \equiv (u_1, u_2, \ldots, u_N)' = (0, u_2, \ldots, u_N)'$ to make subsequent formulas easier to read.

The following Proposition generalizes earlier integral formulas to the N-asset case. All integrals are over $\mathbb{R}^{N-1}$: $\boldsymbol{v}$ is an $(N-1)$-vector. Again, they can be evaluated on the computer. The condition that ensures finiteness of the price of asset j is that $\rho - \boldsymbol{c}(\boldsymbol{e}_j - \boldsymbol{\gamma}/N) > 0$. I assume that this holds for all assets.

Proposition 9. *The price-dividend ratio on asset j is*

$$P/D = e^{-\boldsymbol{\gamma}'\boldsymbol{u}_+/N}\left(e^{u_1}+\cdots+e^{u_N}\right)^{\gamma}\int \frac{\mathscr{F}_{\gamma}^{N}(\boldsymbol{v})e^{i\boldsymbol{u}'\boldsymbol{v}}}{\rho-\boldsymbol{c}(\boldsymbol{e}_j-\boldsymbol{\gamma}/N+i\boldsymbol{U}'\boldsymbol{v})}\,d\boldsymbol{v}\,. \tag{22}$$

Defining the expected return by $ER\,dt \equiv \mathbb{E}(dP + D\,dt)/P$, we have

$$ER = \frac{\Phi}{P/D} + D/P\,,$$

where

$$\Phi = \sum_{\boldsymbol{m}} \binom{\gamma}{\boldsymbol{m}} e^{(\boldsymbol{m}-\boldsymbol{\gamma}/N)'\boldsymbol{u}_+}\int \frac{\mathscr{F}_{\gamma}^{N}(\boldsymbol{v})e^{i\boldsymbol{u}'\boldsymbol{v}}\boldsymbol{c}(\boldsymbol{e}_j+\boldsymbol{m}-\boldsymbol{\gamma}/N+i\boldsymbol{U}'\boldsymbol{v})}{\rho-\boldsymbol{c}(\boldsymbol{e}_j-\boldsymbol{\gamma}/N+i\boldsymbol{U}'\boldsymbol{v})}\,d\boldsymbol{v}\,.$$

The summation is over all vectors $\boldsymbol{m}=(m_1,\ldots,m_N)'$ whose entries are non-negative and add up to γ. I have made use of the multinomial coefficient

$$\binom{\gamma}{\boldsymbol{m}} = \frac{\gamma!}{m_1!\cdots m_N!}\,.$$

The zero-coupon yield to time T is

$$\mathscr{Y}(T) = \rho - \frac{1}{T}\log\left[e^{-\boldsymbol{\gamma}'\boldsymbol{u}_+/N}\left(e^{u_1}+\cdots+e^{u_N}\right)^{\gamma}\int \mathscr{F}_{\gamma}^{N}(\boldsymbol{v})e^{i\boldsymbol{u}'\boldsymbol{v}}e^{\boldsymbol{c}(-\boldsymbol{\gamma}/N+i\boldsymbol{U}'\boldsymbol{v})T}\,d\boldsymbol{v}\right].$$

The riskless rate is

$$r = e^{-\boldsymbol{\gamma}'\boldsymbol{u}_+/N}\left(e^{u_1}+\cdots+e^{u_N}\right)^{\gamma}\int \mathscr{F}_{\gamma}^{N}(\boldsymbol{v})e^{i\boldsymbol{u}'\boldsymbol{v}}\left[\rho-\boldsymbol{c}(-\boldsymbol{\gamma}/N+i\boldsymbol{U}'\boldsymbol{v})\right]\,d\boldsymbol{v}\,.$$

These formulas can be expressed in terms of the dividend shares $\{s_i\}$ by making the substitution $u_k = \log(s_k/s_1)$.

Proof. See Appendix E. □

Figure 13 illustrates how the price-dividend ratio of asset 1 depends on the two state variables s_1 and s_2 in a three-asset example in which the assets have identical and independent fundamentals.

5.1 The robustness of contagion and flight-to-quality

Above, I presented a two-asset calibration in which a small asset experiences a price drop ("contagion") if a large asset has bad dividend news. On the other hand, a sufficiently large asset experiences a *positive* shock when a sufficiently small asset has

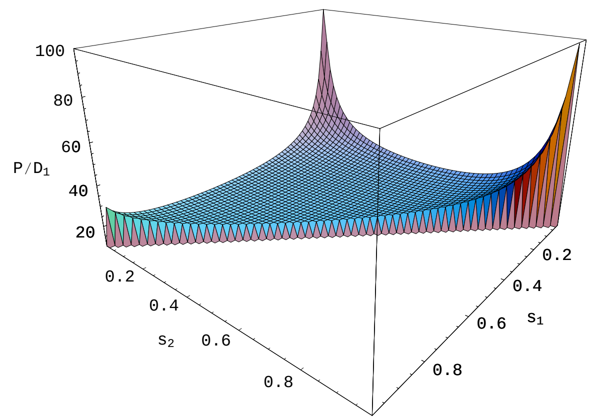

Figure 13: The price-dividend ratio of asset 1 as a function of s_1 and s_2 in a three-asset example.

bad dividend news; this was labelled "flight-to-quality". This effect was dependent on a decrease in the riskless rate outweighing the effect of an increase in the risk premium on the large asset. How robust is this effect? Intuition suggests that with more assets, the riskless rate effect will be muted, while the risk premium effect will continue to matter for individual assets. This section evaluates that intuition.

In the two-asset case, an asset is subject to contagion when its price-dividend ratio is decreasing in its dividend share, and to flight-to-quality when its price-dividend ratio is increasing in its dividend share. In the calibration of Section 3.1, the share, s^*, at which the transition takes place occurs at the minimum point of the price-dividend curve shown in Figure 2b: that is, at $s^* \approx 0.61$.

Alternatively, suppose that there are $N-1$ equally sized small assets and an Nth large asset, and that all assets have independent and identically distributed dividend processes, following geometric Brownian motions with $\mu = 0.02$ and $\sigma = 0.1$. As in the two-asset case, we can calculate the critical dividend share, s^*, above which the Nth asset exhibits flight-to-quality, and below which the Nth asset exhibits contagion, following a negative dividend shock to any one of the $N-1$ small assets.

Table 2 demonstrates that s^* is decreasing in N. An alternative measure of the large asset's relative size at this critical point is the ratio of the its dividend to the dividend of any one of the $N-1$ equally sized small assets. The relative size required for flight-to-quality is increasing in N: when $N = 6$, an asset that has dividends two and a half times as large as any other asset will still experience contagion rather than

N	Critical share, s^*	Relative size
2	0.61	1.56
3	0.48	1.83
4	0.41	2.11
5	0.37	2.38
6	0.35	2.66

Table 2: Above the critical share the large asset experiences flight-to-quality; below, it experiences contagion. Relative size is the ratio of the large asset's dividend to the dividend of one of the small assets, at this critical share.

flight-to-quality, whereas such an asset experiences flight-to-quality if $N \leq 5$. This evidence suggests that when there are several assets of broadly similar size, contagion, not flight-to-quality, is the norm.

5.2 A calibration with three assets

To understand the interactions between (say) the US and UK stock markets, we can follow Campbell (1991) in decomposing unexpected dollar returns into a cashflow news component and a discount-rate news component:

$$\begin{aligned} R_{US,t+1} - \mathbb{E}_t R_{US,t+1} &= CF_{US,t+1} - DR_{US,t+1} \\ R_{UK,t+1} - \mathbb{E}_t R_{UK,t+1} &= CF_{UK,t+1} - DR_{UK,t+1} \end{aligned}$$

Within the equity volatility literature, a stylized fact is that the variance of $R_{US,t+1}$ can largely be attributed to variance of $DR_{US,t+1}$; similarly for the UK. For the purposes of investigating comovement, the covariances or correlations in news terms across the two markets are of interest. Ammer and Mei (1996) conduct just this exercise, using data from the US and UK markets between 1957:1 and 1989:12.[13]

There is more correlation in discount-rate news than in cashflow news. This illustrates what Shiller (1989) described as "excess comovement". Moreover, there is

[13] Ammer and Mei decompose discount-rate news further, into riskless-rate news, excess-return news, and (for the UK) exchange-rate news. I choose to amalgamate these under the heading of discount-rate news and back out the correlations shown in Table 3. This simplifies bringing the model to the data, because within the model discount-rate news is easily calculated by subtracting return news from the unexpected component of log dividend growth (which equals cashflow news because dividend growth is i.i.d.).

Corr	CF_{UK}	DR_{UK}
CF_{US}	0.30	-0.23
DR_{US}	0.36	0.60

Table 3: Correlations backed out from Ammer and Mei (1996).

an intriguing asymmetry in the signs of the off-diagonal entries.

To see what the model predicts, I consider a world with three assets, corresponding to the stock markets of the US, the UK, and the rest of the world. In the interests of simplicity—but at the cost of some realism—I reduce the number of free parameters by assuming that dividends follow geometric Brownian motions with mean log dividend growth equal to 0.02 in each country, and that the volatility of log dividend growth in each country equals 0.112 (a number which I take from Campbell and Cochrane (1999)). In the model, cashflow news is unexpected log dividend growth, so I set the pairwise log dividend growth correlations to 0.30 to match the correlation of US cashflow news with UK cashflow news reported in Table 3. As before, I assume a time preference rate $\rho = 0.03$ and risk aversion $\gamma = 4$.

The only source of asymmetry is in the starting dividend shares of the three assets. I set the initial dividend share of the US to 0.4, of the UK to 0.1, and of the rest of the world to 0.5. These numbers imply that the US starts with a 40.0% share, and the UK with a 11.7% share, of world market capitalization. (Table I of Campbell (1999) reports corresponding market cap shares of 39.9% and 11.9%, respectively, in 1993.) I conduct a Monte Carlo exercise, generating 10,000 sample paths for log dividends in each of the countries. Each sample path corresponds to a 30-year interval, and I use 400 time increments per year. Along each path, I calculate implied dividend shares, price-dividend ratios, and prices. I find realized cashflow news and discount-rate news for each country along each sample path, and compute the correlations corresponding to those in Table 3.

Corr	CF_{UK}	DR_{UK}
CF_{US}	0.30 (0.01)	-0.14 (0.25)
DR_{US}	0.26 (0.08)	0.72 (0.13)

Table 4: Average (and standard deviation) of correlations computed in Monte Carlo simulations of the model.

Table 4 shows the average (and standard deviation) of the resulting correlations. The top left entry is equal to 0.30 by construction. The other three entries are endogenous to the model. The model correctly predicts a high correlation in discount-rate news across the two markets. It also captures the sign change in the off-diagonal entries. Within the model, this sign change can be attributed to the distinction between "flight-to-quality" and "contagion". When the US market experiences bad dividend news, the UK market drops as a result of contagion; this is positive discount-rate news, hence the minus sign in the top right cell. When the UK market experiences bad dividend news, the world is more unbalanced, so riskless rates drop and the US market appreciates, corresponding to negative discount-rate news; hence the plus sign on the correlation in the bottom left cell.

The relatively large standard errors in Table 4 are due to the choice of a 30-year simulation horizon, which was made to facilitate comparison with the results of Ammer and Mei (1996). Performing the same exercise over a two-year horizon gives similar means but roughly halves standard deviations, because there is less time for dividend shares to move far from their starting point.[14]

6 Conclusion

It seems worthwhile to summarize the solution method for readers who are not inclined to look through the appendices. By means of a change of measure followed by a Fourier transform, the Lucas asset-pricing equation (1) is converted into the integral formulas (4) and (22) which can be evaluated numerically.

In the two-asset case, the integral formula (4) can be simplified further if dividends follow geometric Brownian motions. Techniques from complex analysis enable the integral to be expressed as an infinite sum of residues that can be evaluated in closed form, leading to the expression (14). Closed forms are also available in the limit as an asset becomes negligibly small, since then only one residue makes a contribution: the tractable expressions of Section 4 are valid for general dividend processes.

Complicated, interesting, and empirically relevant phenomena emerge from simple assumptions. In various regions of the parameter space, the model exhibits momentum, mean-reversion, contagion, flight to quality, the value-growth effect, and excess

[14]The mean (s.d.) correlation between CF_{US} and CF_{UK} is then 0.30 (0.03); between CF_{US} and DR_{UK} is -0.13 (0.10); between DR_{US} and CF_{UK} is 0.26 (0.05); and between DR_{US} and DR_{UK} is 0.67 (0.07).

volatility. Notably, comovement is a robust feature of the model.

I devote particular attention to the dynamics of a small asset. This case crystallizes the central mechanism of the model particularly clearly and—since the price-dividend ratio of a small asset is sensitively dependent on the state variable—represents a counterpoint to the simple intuition derived from a textbook one-tree model with constant price-dividend ratios. It is also analytically tractable, and various intriguing results emerge. A negligibly small asset whose fundamentals are independent of the rest of the economy may comove endogenously and hence earn a risk premium; and for reasonable parameter values, time variation in the price-dividend ratio of a sufficiently small asset can be attributed entirely to time variation in its expected excess return.

The model closely matches the cross-country correlations between cashflow news and discount-rate news documented in Ammer and Mei (1996). For reasons of space, though, I only conduct a cursory analysis in this paper; it would be desirable to update Ammer and Mei's data and to extend their study to more countries.

There are various other natural directions for further work. First, the analysis of this paper makes it possible to simulate an N-asset economy using dividend growth rates and volatilities calibrated from real data, and therefore to make a more detailed examination of the cross-sectional predictions of the model. Second, the properties of the N-asset integral formulas presented in Proposition 9 might be explored further; attempts to do so may be complicated by the fact that the theory of integration with several complex variables is considerably more involved than that of integration over a single complex variable. Third, the model might be extended in several ways: for example, by introducing Epstein-Zin preferences; by allowing for imperfect substitution between the goods of the trees, in which case real exchange rates enter the picture; or by introducing multiple agents or non-traded goods. Fourth, the equity volatility puzzle remains a puzzle in this paper. A more ambitious extension of this paper might combine the techniques developed here with an approach along Campbell-Cochrane (1999) lines, to investigate interactions between assets in a model that matches observed levels of market volatility.

7 Bibliography

Ammer, J. and J. Mei (1996), "Measuring International Economic Linkages with Stock Market Data," *Journal of Finance*, 51:5:1743–1763.

Andrews, G. E., Askey, R., and R. Roy (1999), *Special Functions*, 1st edition, Cambridge University Press, UK.

Barro, R. J. (2006), "Rare Disasters and Asset Markets in the Twentieth Century," *Quarterly Journal of Economics*, 121:3:823–866.

Billingsley, P. (1995), *Probability and Measure*, 3rd edition, John Wiley & Sons, New York, NY.

Brainard, W. C. and J. Tobin (1968), "Pitfalls in Financial Model Building," *American Economic Review*, 58:2:99–122.

Brainard, W. C. and J. Tobin (1992), "On the Internationalization of Portfolios," *Oxford Economic Papers*, 44:533–565.

Breeden, D. T. (1979), "An Intertemporal Asset Pricing Model with Stochastic Consumption and Investment Opportunities," *Journal of Financial Economics*, 7:265–296.

Campbell, J. Y. (1991), "A Variance Decomposition for Stock Returns," *Economic Journal*, 101:157–179.

Campbell, J. Y. (1999), "Asset Prices, Consumption, and the Business Cycle," Chapter 19 in J. B. Taylor and M. Woodford eds., *Handbook of Macroeconomics Vol. 1*, North-Holland, Amsterdam, 1231–1303.

Campbell, J. Y. and J. H. Cochrane (1999), "By Force of Habit: A Consumption-Based Explanation of Aggregate Stock Market Behavior," *Journal of Political Economy*, 107:2:205–251.

Cochrane, J. H. (2005), *Asset Pricing*, revised edition, Princeton University Press, Princeton, NJ.

Cochrane, J. H., Longstaff, F. A., and P. Santa-Clara (2008), "Two Trees," *Review of Financial Studies*, 21:1:347–385.

Cohen, R. B., Polk, C., and T. Vuolteenaho (2003), "The Value Spread," *Journal of Finance*, 58:2:609–641.

Cole, H. L. and M. Obstfeld (1991), "Commodity Trade and International Risk Sharing," *Journal of Monetary Economics*, 28:3–24.

Cont, R. and P. Tankov (2004), *Financial Modelling with Jump Processes*, Chapman & Hall/CRC, Boca Raton, FL.

Cox, J. C., Ingersoll, J. E., and S. A. Ross (1985), "An Intertemporal General Equilibrium Model of Asset Prices," *Econometrica*, 53:2:363–384.

Duffee, G. R. (2005), "Time Variation in the Covariance between Stock Returns and Consumption Growth," *Journal of Finance*, 60:4:1673–1712.

Fama, E. F. and K. R. French (1989), "Business Conditions and Expected Returns on Stocks and Bonds," *Journal of Financial Economics*, 25:23–49.

Fama, E. F. and K. R. French (1993), "Common Risk Factors in the Returns on Stocks and Bonds," *Journal of Financial Economics*, 33:131–155.

Forbes, K. J. and R. Rigobon (2002), "No Contagion, Only Interdependence: Measuring Stock Market Comovements," *Journal of Finance*, 57:5:2223–2261.

Gabaix, X. (2008), "Variable Rare Disasters: A Tractable Theory of Ten Puzzles in Macro-Finance," *American Economic Review*, forthcoming.

Lucas, R. E. (1978), "Asset Prices in an Exchange Economy," *Econometrica*, 46:6:1429–1445.

Lucas, R. E. (1982), "Interest Rates and Currency Prices in a Two-Country World," *Journal of Monetary Economics*, 10:335–359.

Martin, I. W. R. (2008), "Consumption-Based Asset Pricing with Higher Cumulants," working paper.

Mehra, R. and E. C. Prescott (1985), "The Equity Premium: A Puzzle," *Journal of Monetary Economics*, 15:145–161.

Menzly, L., Santos, T., and P. Veronesi (2004), "Understanding Predictability," *Journal of Political Economy*, 112:1:1–47.

Merton, R. C. (1973), "An Intertemporal Capital Asset Pricing Model," *Econometrica*, 41:5:867–887.

Pástor, L. and P. Veronesi (2003), "Stock Valuation and Learning about Profitability," *Journal of Finance*, 58:5:1749–1789.

Pástor, L. and P. Veronesi (2006), "Was there a Nasdaq Bubble in the Late 1990s?" *Journal of Financial Economics*, 81:61–100.

Pavlova, A. and R. Rigobon (2007), "Asset Prices and Exchange Rates," *Review of Financial Studies*, 20:4:1139–1181.

Rietz, T. A. (1988), "The Equity Premium: A Solution," *Journal of Monetary Economics*, 22:117–131.

Rogers, L. C. G., and D. Williams (2000), *Diffusions, Markov Processes, and Martingales, Volume 1*, Cambridge University Press, Cambridge, UK.

Santos, T. and P. Veronesi (2006), "Labor Income and Predictable Stock Returns," *Review of Financial Studies*, 19:1:1–44.

Sato, K. (1999), *Lévy Processes and Infinitely Divisible Distributions*, 1st edition, Cambridge University Press, Cambridge, UK.

Shiller, R. J. (1981), "Do Stock Prices Move Too Much to be Justified by Subsequent Changes in Dividends?" *American Economic Review*, 71:421–436.

Shiller, R. J. (1989), "Comovements in Stock Prices and Comovements in Dividends," *Journal of Finance*, 44:3:719–729.

Slater, L. J. (1966), *Generalized Hypergeometric Functions*, Cambridge University Press, Cambridge, UK.

A General solution in the two-asset case

A.1 Preliminary mathematical results

A.1.1 An expectation

This section contains a calculation used in the proof of Proposition 1. The goal is to evaluate

$$E \equiv \mathbb{E}\left(\frac{e^{\alpha_1 \widetilde{y}_{1t}+\alpha_2 \widetilde{y}_{2t}}}{\left[e^{y_{10}+\widetilde{y}_{1t}}+e^{y_{20}+\widetilde{y}_{2t}}\right]^{\gamma}}\right)$$

for general $\alpha_1, \alpha_2, \gamma > 0$. First, I rewrite the expectation, noting that

$$\begin{aligned}\mathbb{E}\left(\frac{e^{\alpha_1 \widetilde{y}_{1t}+\alpha_2 \widetilde{y}_{2t}}}{\left[e^{y_{10}+\widetilde{y}_{1t}}+e^{y_{20}+\widetilde{y}_{2t}}\right]^{\gamma}}\right) &= e^{-\gamma/2(y_{10}+y_{20})} \times \\ &\quad \mathbb{E}\left(\frac{e^{(\alpha_1-\gamma/2)\widetilde{y}_{1t}+(\alpha_2-\gamma/2)\widetilde{y}_{2t}}}{\left[2\cosh((y_{20}-y_{10}+\widetilde{y}_{2t}-\widetilde{y}_{1t})/2)\right]^{\gamma}}\right) \qquad (23)\end{aligned}$$

To take care of the exponential in the numerator inside the expectation, I transform the probability law, defining

$$\widetilde{\mathbb{E}}\left[Y\right] \equiv e^{-t\boldsymbol{c}(\alpha_1-\gamma/2,\alpha_2-\gamma/2)} \cdot \mathbb{E}\left[e^{(\alpha_1-\gamma/2)\widetilde{y}_{1t}+(\alpha_2-\gamma/2)\widetilde{y}_{2t}} \cdot Y\right] . \qquad (24)$$

This is an Esscher transform of the original law, and it has the property that

$$\widetilde{\boldsymbol{c}}(v_1, v_2) \equiv \log \widetilde{\mathbb{E}}\left[e^{v_1 \widetilde{y}_{11}+v_2 \widetilde{y}_{21}}\right] = \boldsymbol{c}(\alpha_1-\gamma/2+v_1, \alpha_2-\gamma/2+v_2) - \boldsymbol{c}(\alpha_1-\gamma/2, \alpha_2-\gamma/2) . \qquad (25)$$

In terms of this transformed law, the right hand side of (23) equals

$$e^{-\gamma(y_{10}+y_{20})/2+\boldsymbol{c}(\alpha_1-\gamma/2,\alpha_2-\gamma/2)t}\,\widetilde{\mathbb{E}}\left(\frac{1}{\left[2\cosh((y_{20}-y_{10}+\widetilde{y}_{2t}-\widetilde{y}_{1t})/2)\right]^{\gamma}}\right) \qquad (26)$$

To make further progress, we can now attack the expectation in (26) by exploiting the fact that $1/\left[2\cosh(u/2)\right]^{\gamma}$ has a Fourier transform which can be found in closed form for integer $\gamma > 0$. Define the Fourier transform $\mathscr{F}_{\gamma}(v)$ by

$$\frac{1}{\left[2\cosh(u/2)\right]^{\gamma}} = \int_{-\infty}^{\infty} e^{iuv} \mathscr{F}_{\gamma}(v)\, dv \qquad (27)$$

We have, then,

$$
\begin{aligned}
E &= e^{-\gamma(y_{10}+y_{20})/2+\boldsymbol{c}(\alpha_1-\gamma/2,\alpha_2-\gamma/2)t}\, \widetilde{\mathbb{E}}\left(\int_{-\infty}^{\infty} e^{iv(y_{20}-y_{10}+\widetilde{y}_{2t}-\widetilde{y}_{1t})}\mathscr{F}_\gamma(v)\,dv\right) \\
&= e^{-\gamma(y_{10}+y_{20})/2+\boldsymbol{c}(\alpha_1-\gamma/2,\alpha_2-\gamma/2)t}\left(\int_{-\infty}^{\infty} e^{\widetilde{\boldsymbol{c}}(-iv,iv)t}\cdot e^{iv(y_{20}-y_{10})}\mathscr{F}_\gamma(v)\,dv\right) \\
&= e^{-\gamma(y_{10}+y_{20})/2}\int_{-\infty}^{\infty} e^{\boldsymbol{c}(\alpha_1-\gamma/2-iv,\alpha_2-\gamma/2+iv)t}\cdot e^{iv(y_{20}-y_{10})}\mathscr{F}_\gamma(v)\,dv\,. \qquad (28)
\end{aligned}
$$

A.1.2 The Fourier transform $\mathscr{F}_\gamma(v)$

By the Fourier inversion theorem, definition (27) implies that

$$
\begin{aligned}
\mathscr{F}_\gamma(v) &= \frac{1}{2\pi}\int_{-\infty}^{\infty}\frac{e^{-iuv}}{(2\cosh(u/2))^\gamma}\,du \\
&= \frac{1}{2\pi}\int_{-\infty}^{\infty}\frac{e^{-iuv}}{\left(e^{u/2}+e^{-u/2}\right)^\gamma}\,du\,. \qquad (29)
\end{aligned}
$$

Make the change of variable $u=\log\left[t/(1-t)\right]$. It follows that

$$du=\frac{dt}{t(1-t)}$$

so on making this substitution in (29), we have

$$
\begin{aligned}
\mathscr{F}_\gamma(v) &= \frac{1}{2\pi}\int_0^1 \frac{\left(\frac{t}{1-t}\right)^{-iv}}{\left(\sqrt{\frac{t}{1-t}}+\sqrt{\frac{1-t}{t}}\right)^\gamma}\,\frac{dt}{t(1-t)} \\
&= \frac{1}{2\pi}\int_0^1 t^{\gamma/2-iv}(1-t)^{\gamma/2+iv}\frac{dt}{t(1-t)}\,.
\end{aligned}
$$

This is a Dirichlet surface integral. As shown in Andrews, Askey and Roy (1999, p. 34), it can be evaluated in terms of Γ-functions, giving

$$\mathscr{F}_\gamma(v)=\frac{1}{2\pi}\frac{\Gamma(\gamma/2-iv)\Gamma(\gamma/2+iv)}{\Gamma(\gamma)}\,. \qquad (30)$$

For future reference, it is useful to note an equivalent representation of $\mathscr{F}_\gamma(v)$. Contour integration reveals that $\mathscr{F}_1(v)=\frac{1}{2}\mathrm{sech}\pi v$ and $\mathscr{F}_2(v)=\frac{1}{2}v\,\mathrm{cosech}\pi v$. From these two facts, expression (30), and the fact that $\Gamma(x)=(x-1)\Gamma(x-1)$, it follows that for positive integer γ, we have

$$
\mathscr{F}_\gamma(v)=\begin{cases}
\dfrac{v\,\mathrm{cosech}(\pi v)}{2(\gamma-1)!}\cdot\displaystyle\prod_{n=1}^{\gamma/2-1}\left(v^2+n^2\right) & \text{for even } \gamma\,, \\[2ex]
\dfrac{\mathrm{sech}(\pi v)}{2(\gamma-1)!}\cdot\displaystyle\prod_{n=1}^{(\gamma-1)/2}\left(v^2+(n-1/2)^2\right) & \text{for odd } \gamma\,.
\end{cases} \qquad (31)
$$

A.1.3 An Itô calculation

Given a jump-diffusion $\boldsymbol{y}$, with $d\boldsymbol{y} = \boldsymbol{\mu}dt + \boldsymbol{A}d\boldsymbol{Z} + \boldsymbol{J}dN$, this section seeks a simple formula for $\mathbb{E}d(e^{\boldsymbol{w}'\boldsymbol{y}})$, where $\boldsymbol{w}$ is a constant vector. First, define $x \equiv \boldsymbol{w}'\boldsymbol{y}$; then $dx = \boldsymbol{w}'\boldsymbol{\mu}dt + \boldsymbol{w}'\boldsymbol{A}d\boldsymbol{Z} + \boldsymbol{w}'\boldsymbol{J}dN$. We seek $\mathbb{E}d(e^x)$. By Itô's formula for jump-diffusions, we have

$$d(e^x) = e^x\left[\left(\boldsymbol{w}'\boldsymbol{\mu} + \frac{1}{2}\boldsymbol{w}'\boldsymbol{\Sigma}\boldsymbol{w}\right)dt + \boldsymbol{w}'\boldsymbol{A}d\boldsymbol{Z} + \left(e^{\boldsymbol{w}'\boldsymbol{J}} - 1\right)dN\right]$$

where $\boldsymbol{\Sigma} \equiv \boldsymbol{A}\boldsymbol{A}'$; and so, after taking expectations,

$$\begin{aligned}\mathbb{E}d(e^{\boldsymbol{w}'\boldsymbol{y}}) &= e^{\boldsymbol{w}'\boldsymbol{y}}\cdot\left[\boldsymbol{w}'\boldsymbol{\mu} + \frac{1}{2}\boldsymbol{w}'\boldsymbol{\Sigma}\boldsymbol{w} + \omega\left(\mathbb{E}e^{\boldsymbol{w}'\boldsymbol{J}} - 1\right)\right]dt \\ &= e^{\boldsymbol{w}'\boldsymbol{y}}\cdot\boldsymbol{c}(\boldsymbol{w})dt\,. \end{aligned} \tag{32}$$

In the case in which $\boldsymbol{y}$ is a general Lévy process, (32) holds by Proposition 8.20 of Cont and Tankov (2004).

A.2 Returns

We have

$$P_{\boldsymbol{\alpha}} = (D_{10} + D_{20})^{\gamma}\, e^{(\alpha_1-\gamma/2)y_{10}+(\alpha_2-\gamma/2)y_{20}}\int_{-\infty}^{\infty}\frac{e^{iv(y_{20}-y_{10})}\mathscr{F}_{\gamma}(v)}{\rho - \boldsymbol{c}(\alpha_1-\gamma/2-iv, \alpha_2-\gamma/2+iv)}\,dv$$

For convenience, I write, throughout this section,

$$h(v) \equiv \frac{\mathscr{F}_{\gamma}(v)}{\rho - \boldsymbol{c}(\alpha_1-\gamma/2-iv, \alpha_2-\gamma/2+iv)} \quad \text{and} \quad \binom{n}{m} \equiv \frac{n!}{m!(n-m)!}.$$

Introducing this notation,

$$\begin{aligned} P_{\boldsymbol{\alpha}} &= \int_{-\infty}^{\infty} h(v)\cdot(e^{y_{10}} + e^{y_{20}})^{\gamma}\, e^{(\alpha_1-\gamma/2-iv)y_{10}+(\alpha_2-\gamma/2+iv)y_{20}}\,dv \\ &= \int_{-\infty}^{\infty} h(v)\cdot\sum_{m=0}^{\gamma}\left[\binom{\gamma}{m}e^{my_{10}}\cdot e^{(\gamma-m)y_{20}}\right]e^{(\alpha_1-\gamma/2-iv)y_{10}+(\alpha_2-\gamma/2+iv)y_{20}}\,dv \\ &= \sum_{m=0}^{\gamma}\binom{\gamma}{m}\int_{-\infty}^{\infty} h(v)\cdot e^{(\alpha_1-\gamma/2+m-iv)y_{10}+(\alpha_2+\gamma/2-m+iv)y_{20}}\,dv \\ &\equiv \sum_{m=0}^{\gamma}\binom{\gamma}{m}\int_{-\infty}^{\infty} h(v)\cdot e^{\boldsymbol{w}_m(v)\cdot\boldsymbol{y}}\,dv\,, \end{aligned} \tag{33}$$

where

$$\boldsymbol{w}_m(v) \equiv (\alpha_1 - \gamma/2 + m - iv, \alpha_2 + \gamma/2 - m + iv)'$$

The calculation of Appendix A.1.3, above, can now be used in (33) to show that

$$\mathbb{E}(dP_{\boldsymbol{\alpha}}) = \left\{ \sum_{m=0}^{\gamma} \binom{\gamma}{m} \int_{-\infty}^{\infty} h(v) \cdot e^{\boldsymbol{w}_m(v)\cdot \boldsymbol{y}} \boldsymbol{c}\left[\boldsymbol{w}_m(v)\right] \, dv \right\} \cdot dt$$

Dividing by (33) and rearranging, the expected capital gain is given by the formula

$$\frac{\mathbb{E}dP_{\boldsymbol{\alpha}}}{P_{\boldsymbol{\alpha}}} = \frac{\displaystyle\sum_{m=0}^{\gamma} \binom{\gamma}{m} e^{-mu} \int_{-\infty}^{\infty} h(v) e^{iuv} \cdot \boldsymbol{c}(\boldsymbol{w}_m(v)) \, dv}{\displaystyle\sum_{m=0}^{\gamma} \binom{\gamma}{m} e^{-mu} \int_{-\infty}^{\infty} h(v) e^{iuv} \, dv} \cdot dt$$

A.3 Real interest rates

From the Euler equation, we have

$$\begin{aligned} B_T &= \mathbb{E}\left[e^{-\rho T} \left(\frac{C_T}{C_0} \right)^{-\gamma} \right] \\ &= e^{-\rho T} C_0^{\gamma} \mathbb{E}\left[\frac{1}{(D_{1T} + D_{2T})^{\gamma}} \right] \end{aligned}$$

Using the result of Appendix A.1.1, we find that

$$\begin{aligned} B_T &= e^{-\rho T} \left(e^{y_{10}} + e^{y_{20}} \right)^{\gamma} e^{-\gamma(y_{10}+y_{20})/2} \int_{-\infty}^{\infty} e^{iv(y_{20}-y_{10})} \mathscr{F}_{\gamma}(v) e^{\mathbf{c}(-\gamma/2-iv,-\gamma/2+iv)T} \, dv \\ &= e^{-\rho T} \left[2\cosh(u/2) \right]^{\gamma} \int_{-\infty}^{\infty} \mathscr{F}_{\gamma}(v) e^{iuv} \cdot e^{\mathbf{c}(-\gamma/2-iv,-\gamma/2+iv)T} \, dv \, , \end{aligned}$$

as claimed. The yield, $\mathscr{Y}(T)$, follows directly from this expression:

$$\mathscr{Y}(T) = \rho - \frac{1}{T} \log \left\{ \left[2\cosh(u/2) \right]^{\gamma} \int_{-\infty}^{\infty} \mathscr{F}_{\gamma}(v) e^{iuv} \cdot e^{\mathbf{c}(-\gamma/2-iv,-\gamma/2+iv)T} \, dv \right\} . \quad (34)$$

The riskless rate is found by taking the limit as $T \downarrow 0$ in (34). To calculate this limit, first use the fact that

$$\left[2\cosh(u/2) \right]^{\gamma} \int_{-\infty}^{\infty} \mathscr{F}_{\gamma}(v) e^{iuv} \, dv = 1$$

to rewrite equation (34) as

$$\mathscr{Y}(T) = \rho - \frac{1}{T}\log\left\{1 + [2\cosh(u/2)]^{\gamma}\int_{-\infty}^{\infty}\mathscr{F}_{\gamma}(v)e^{iuv}\left[e^{\boldsymbol{c}(-\gamma/2-iv,-\gamma/2+iv)T} - 1\right]\,dv\right\}.$$

It follows, by L'Hôpital's rule, that

$$\begin{aligned} r &= \rho - [2\cosh(u/2)]^{\gamma}\int_{-\infty}^{\infty}\mathscr{F}_{\gamma}(v)e^{iuv}\boldsymbol{c}(-\gamma/2-iv,-\gamma/2+iv)\,dv \\ &= [2\cosh(u/2)]^{\gamma}\int_{-\infty}^{\infty}\mathscr{F}_{\gamma}(v)e^{iuv}\cdot[\rho - \boldsymbol{c}(-\gamma/2-iv,-\gamma/2+iv)]\,dv. \end{aligned}$$

B The ridge property

This section expands on two closely related issues. First, it demonstrates that

$$\rho - \mathrm{Re}[\boldsymbol{c}(\alpha_1 - \gamma/2 - iv, \alpha_2 - \gamma/2 + iv)] > 0 \quad \text{for all } v \in \mathbb{R}$$

follows from the apparently weaker assumption that the inequality holds at $v = 0$. Second, it considers the problem of finding the zero of $\rho - \boldsymbol{c}(\alpha_1 - \gamma/2 - iv, \alpha_2 - \gamma/2 + iv)$ in the upper half-plane which is closest to the real axis (the *minimal* zero, in the terminology of Appendix D), which is relevant in the small-asset limit.

In each case, we are interested in the properties of $\boldsymbol{c}(\alpha_1 - \gamma/2 - iv, \alpha_2 - \gamma/2 + iv)$, considered as a function of v. Recalling the change of measure of Appendix A.1.1, we can exploit the fact that

$$\boldsymbol{c}(\alpha_1 - \gamma/2 - iv, \alpha_2 - \gamma/2 + iv) = \widetilde{\boldsymbol{c}}(-iv, iv) + \boldsymbol{c}(\alpha_1 - \gamma/2, \alpha_2 - \gamma/2)$$

where $\widetilde{\boldsymbol{c}}(v_1, v_2)$ is the CGF under the changed measure. Next, note that

$$\widetilde{\boldsymbol{c}}(-iv, iv) = \log\widetilde{\mathbb{E}}\,e^{iv(\widetilde{y}_{21} - \widetilde{y}_{11})} \equiv \log\psi(v)$$

which defines $\psi(v)$ as the characteristic function of the random variable $\widetilde{y}_{21} - \widetilde{y}_{11}$.

The characteristic function ψ has the *ridge property*: for real v and w, we have

$$|\psi(v + iw)| \leq |\psi(iw)|\,.$$

This follows because (writing X for $\widetilde{y}_{21} - \widetilde{y}_{11}$)

$$|\psi(v + iw)| = \left|\widetilde{\mathbb{E}}\,e^{iX(v+iw)}\right| \leq \widetilde{\mathbb{E}}\left|e^{iX(v+iw)}\right| = \widetilde{\mathbb{E}}\,e^{-wX} = \psi(iw) = |\psi(iw)|\,.$$

Proposition 10. *The assumption that*

$$\rho - Re[\boldsymbol{c}(\alpha_1 - \gamma/2 - iv, \alpha_2 - \gamma/2 + iv)] > 0 \quad \textit{for all } v \in \mathbb{R}.$$

follows from the apparently weaker assumption that the inequality holds at $v = 0$:

$$\rho - \boldsymbol{c}(\alpha_1 - \gamma/2, \alpha_2 - \gamma/2) > 0\,. \tag{35}$$

Proof. Suppose the apparently weaker inequality holds. In terms of the characteristic function ψ, we have

$$\rho - \boldsymbol{c}(\alpha_1 - \gamma/2 - iv, \alpha_2 - \gamma/2 + iv) = \rho - \boldsymbol{c}(\alpha_1 - \gamma/2, \alpha_2 - \gamma/2) - \log \psi(v). \tag{36}$$

So, for $v \in \mathbb{R}$, we have

$$\begin{aligned}
\rho - \mathrm{Re}[\boldsymbol{c}(\alpha_1 - \gamma/2 - iv, \alpha_2 - \gamma/2 + iv)] &= \rho - \boldsymbol{c}(\alpha_1 - \gamma/2, \alpha_2 - \gamma/2) - \mathrm{Re}\log\psi(v) \\
&= \rho - \boldsymbol{c}(\alpha_1 - \gamma/2, \alpha_2 - \gamma/2) - \log|\psi(v)| \\
&\geq \rho - \boldsymbol{c}(\alpha_1 - \gamma/2, \alpha_2 - \gamma/2) - \log|\psi(0)| \\
&= \rho - \boldsymbol{c}(\alpha_1 - \gamma/2, \alpha_2 - \gamma/2) \\
&> 0 \quad \text{by assumption,}
\end{aligned}$$

which establishes the claim. The first inequality follows by the ridge property. □

Under assumption (35) this proposition implies, for example, that there are no zeros of $\rho - \boldsymbol{c}(\alpha_1 - \gamma/2 - iv, \alpha_2 - \gamma/2 + iv)$ *on* the real axis. The following proposition documents an important property of the closest zero above the real axis.

Proposition 11. *Consider*

$$\rho - \boldsymbol{c}(\alpha_1 - \gamma/2 - iv, \alpha_2 - \gamma/2 + iv) \tag{37}$$

as a function of $v \in \mathbb{C}$, and suppose that the condition

$$\rho - \boldsymbol{c}(\alpha_1 - \gamma/2, \alpha_2 - \gamma/2) > 0 \tag{38}$$

holds. Then the zero of (37) *in the upper half-plane which is closest to the real axis lies on the imaginary axis.*

Proof. Using equation (36) above, any zero, z, satisfies

$$\rho - \boldsymbol{c}(\alpha_1 - \gamma/2, \alpha_2 - \gamma/2) = \log \psi(z)\,.$$

Writing the left-hand side as $\widehat{\rho} \in \mathbb{R}$ for convenience, any zero z must satisfy $\psi(z) = \exp \widehat{\rho}$. The fact that $\widehat{\rho} > 0$ follows from (38).

Let z^* be the zero in the upper half-plane with smallest imaginary part, and suppose (for a contradiction) that $\operatorname{Re} z^* \neq 0$. Let $\widetilde{z} = (\operatorname{Im} z^*)i$ be the projection of z^* onto the imaginary axis. By the ridge property, we have $\psi(\widetilde{z}) > |\psi(z^*)| = \exp \widehat{\rho}$. So, $\psi(\widetilde{z}) > \exp \widehat{\rho} > 1 = \psi(0)$. By continuity of ψ, there must be a purely imaginary $\widehat{z}$ which lies between 0 and $\widetilde{z}$ and satisfies $\psi(\widehat{z}) = \exp \widehat{\rho}$—but this contradicts the assumption that z^* had smallest imaginary part. Therefore the zero with smallest imaginary part must, in fact, lie on the imaginary axis. □

C The Brownian motion case

From (6), the price-dividend ratio on the $\boldsymbol{\alpha}$-asset is

$$P/D(u) = [2\cosh(u/2)]^{\gamma} \cdot \int_{-\infty}^{\infty} \frac{e^{iuv} \mathscr{F}_{\gamma}(v)}{\rho - \boldsymbol{c}(\alpha_1 - \gamma/2 - iv, \alpha_2 - \gamma/2 + iv)} \, dv \,. \tag{39}$$

In this Brownian motion case,

$$\boldsymbol{c}(\theta_1, \theta_2) = \mu_1\theta_1 + \mu_2\theta_2 + \frac{1}{2}\sigma_{11}\theta_1^2 + \sigma_{12}\theta_1\theta_2 + \frac{1}{2}\sigma_{22}\theta_2^2 \,.$$

There are two solutions to the equation $\rho - \boldsymbol{c}(\alpha_1 - \gamma/2 - iv, \alpha_2 - \gamma/2 + iv) = 0$, each of which lies on the imaginary axis. One—call it $\lambda_1 i$—lies in the upper half-plane; the other—call it $\lambda_2 i$—lies in the lower half-plane. We can rewrite

$$\rho - \boldsymbol{c}(\alpha_1 - \gamma/2 - iv, \alpha_2 - \gamma/2 + iv) = B(v - \lambda_1 i)(v - \lambda_2 i)$$

for some $B > 0, \lambda_1 > 0, \lambda_2 < 0$. (I establish the claims made in this paragraph in Step 5, below.)

The aim, then, is to evaluate

$$I \equiv \int_{-\infty}^{\infty} \frac{e^{iuv} \mathscr{F}_{\gamma}(v)}{B(v - \lambda_1 i)(v - \lambda_2 i)} \, dv \,, \tag{40}$$

in terms of which the price-dividend ratio is

$$P/D = [2\cosh(u/2)]^{\gamma} \cdot I \,. \tag{41}$$

The proof of Proposition 4, which amounts to evaluating the integral (40), is somewhat involved, so I have divided it into several steps. Step 1 starts from the assumption that the state variable u is positive—an assumption that will later be relaxed—and demonstrates that the integral (39) can be calculated via the Cauchy's Residue Theorem. Steps 2 and 3 carry out these calculations and simplify. Step 4 demonstrates that the resulting expression is also valid for negative u. Step 5 calculates B, λ_1, and λ_2 in terms of fundamental parameters, which concludes the proof.

Step 1. Let $u > 0$. Consider the case in which γ is even. Let $R_n \equiv n + 1/2$, where n is an integer. Define the large semicircle Ω_n to be the semicircle whose base lies along the real axis from $-R_n$ to R_n and which has a semicircular arc (ω_n) passing through the upper half-plane from R_n through $R_n i$ and back to $-R_n$. I will first show that

$$I = \lim_{n\to\infty} \int_{\Omega_n} \frac{e^{iuv}\mathscr{F}_\gamma(v)}{B(v-\lambda_1 i)(v-\lambda_2 i)}\, dv\,. \tag{42}$$

Then, from the residue theorem, it will follow that

$$I = 2\pi i \cdot \sum \operatorname{Res}\left\{ \frac{e^{iuv}\mathscr{F}_\gamma(v)}{B(v-\lambda_1 i)(v-\lambda_2 i)}; v_p \right\}\,, \tag{43}$$

where the sum is taken over all poles v_p in the upper half-plane.

The first step is to establish that (42) holds. The right-hand side is equal to

$$\lim_{n\to\infty} \quad \underbrace{\int_{-R_n}^{R_n} \frac{e^{iuv}\mathscr{F}_\gamma(v)}{B(v-\lambda_1 i)(v-\lambda_2 i)}\, dv}_{I_n} + \underbrace{\int_{\omega_n} \frac{e^{iuv}\mathscr{F}_\gamma(v)}{B(v-\lambda_1 i)(v-\lambda_2 i)}\, dv}_{J_n}$$

The integral I_n tends to I as n tends to infinity. The aim, then, is to establish that the second term J_n tends to zero as n tends to infinity. Along the arc ω_n, we have $v = R_n e^{i\theta}$ where θ varies between 0 and π.

At this point of the argument it is convenient to work with the representation of $\mathscr{F}_\gamma(v)$ of equation (31). Substituting from (31), we have

$$J_n = \int_0^\pi \frac{e^{iuR_n\cos\theta - uR_n\sin\theta}P(R_n e^{i\theta})}{Q(R_n e^{i\theta})\left(e^{\pi R_n(\cos\theta + i\sin\theta)} - e^{-\pi R_n(\cos\theta + i\sin\theta)}\right)} \cdot R_n i e^{i\theta}\, d\theta$$

with $P(\cdot)$ and $Q(\cdot)$ polynomials.

To show that J_n tends to zero as n tends to infinity, I separate the range of integration $[0,\pi]$ into two parts: $[\pi/2 - \delta, \pi/2 + \delta]$ and its complement in $[0,\pi]$. Here δ will be chosen to be extremely small.

First, consider

$$\begin{aligned} J_n^{(1)} &\equiv \left| \int_{\pi/2-\delta}^{\pi/2+\delta} \frac{P(R_n e^{i\theta}) e^{iuR_n\cos\theta - uR_n\sin\theta} R_n i e^{i\theta}}{Q(R_n e^{i\theta})\left(e^{\pi R_n(\cos\theta + i\sin\theta)} - e^{-\pi R_n(\cos\theta+i\sin\theta)}\right)} \, d\theta \right| \\ &\leq \int_{\pi/2-\delta}^{\pi/2+\delta} \left| \frac{P(R_n e^{i\theta})}{Q(R_n e^{i\theta})} \right| \frac{e^{-uR_n\sin\theta} R_n}{\left| e^{\pi R_n(\cos\theta+i\sin\theta)} - e^{-\pi R_n(\cos\theta+i\sin\theta)} \right|} \, d\theta \end{aligned}$$

Pick δ sufficiently small that

$$\left| e^{\pi R_n(\cos\theta+i\sin\theta)} - e^{-\pi R_n(\cos\theta+i\sin\theta)} \right| \geq 2 - \varepsilon$$

for all $\theta \in [\pi/2 - \delta, \pi/2 + \delta]$; ε is some very small number close to but greater than zero. This is possible because the left-hand side is continuous and equal to 2 when $\theta = \pi/2$. Then,

$$J_n^{(1)} \leq \int_{\pi/2-\delta}^{\pi/2+\delta} \left| \frac{P(R_n e^{i\theta})}{Q(R_n e^{i\theta})} \right| \frac{e^{-uR_n\sin\theta} R_n}{2 - \varepsilon} \, d\theta \tag{44}$$

Since

(i) we can also ensure that δ is small enough that $\sin\theta \geq \varepsilon$ for θ in the range of integration,

(ii) $|P(R_n e^{i\theta})| \leq P_2(R_n)$, where P_2 is the polynomial obtained by taking absolute values of the coefficients in P,

(iii) $Q(R_n e^{i\theta})$ tends to infinity as R_n becomes large, and

(iv) decaying exponentials decay faster than polynomials grow, in the sense that for any positive k and λ, $x^k e^{-\lambda x} \to 0$ as $x \to \infty$, $x \in \mathbb{R}$,

we see, finally, that the right-hand side of (44), and hence $J_n^{(1)}$, tends to zero as n tends to infinity,

It remains to be shown that

$$J_n^{(2)} \equiv \left| \int_{[0,\pi/2-\delta]\cup[\pi/2+\delta,\pi]} \frac{P(R_n e^{i\theta}) e^{iuR_n\cos\theta - uR_n\sin\theta} R_n i e^{i\theta}}{Q(R_n e^{i\theta})\left(e^{\pi R_n(\cos\theta + i\sin\theta)} - e^{-\pi R_n(\cos\theta+i\sin\theta)}\right)} \, d\theta \right|$$

is zero in the limit. Since $\delta > 0$, for all θ in the range of integration we have that $|\cos\theta| \geq \zeta > 0$, for some small ζ. We have

$$J_n^{(2)} \leq \int_{[0,\pi/2-\delta]\cup[\pi/2+\delta,\pi]} \left| \frac{P(R_n e^{i\theta})}{Q(R_n e^{i\theta})} \right| \frac{e^{-uR_n\sin\theta} R_n}{\left| e^{\pi R_n(\cos\theta+i\sin\theta)} - e^{-\pi R_n(\cos\theta+i\sin\theta)} \right|} \, d\theta \,.$$

Now,

$$\begin{aligned}
& \left|e^{\pi R_n(\cos\theta + i\sin\theta)} - e^{-\pi R_n(\cos\theta+i\sin\theta)}\right| \\
\geq \ & \left|\left|e^{\pi R_n(\cos\theta + i\sin\theta)}\right| - \left|e^{-\pi R_n(\cos\theta+i\sin\theta)}\right|\right| \\
= \ & e^{\pi R_n|\cos\theta|} - e^{-\pi R_n|\cos\theta|} \\
\geq \ & e^{\pi R_n\zeta} - e^{-\pi R_n\zeta}
\end{aligned}$$

for all θ in the range of integration. So,

$$\begin{aligned}
J_n^{(2)} \ & \leq \ \int_{[0,\pi/2-\delta]\cup[\pi/2+\delta,\pi]} \left|\frac{P(R_n e^{i\theta})}{Q(R_n e^{i\theta})}\right| \frac{e^{-uR_n\sin\theta} R_n}{e^{\pi R_n\zeta} - e^{-\pi R_n\zeta}}\, d\theta \\
& \leq \ \int_{[0,\pi/2-\delta]\cup[\pi/2+\delta,\pi]} \left|\frac{P(R_n e^{i\theta})}{Q(R_n e^{i\theta})}\right| \frac{R_n}{e^{\pi R_n\zeta} - e^{-\pi R_n\zeta}}\, d\theta
\end{aligned}$$

which tends to zero as n tends to infinity.

The case of γ odd is almost identical. The only important difference is that we take $R_n = n$ (as opposed to $n + 1/2$) before allowing n to go to infinity. The reason for doing so is that we must take care to avoid the poles of $\mathscr{F}_\gamma(v)$ on the imaginary axis.

Step 2. From now on, I revert to the definition of $\mathscr{F}_\gamma(v)$ as

$$\mathscr{F}_\gamma(v) = \frac{1}{2\pi}\frac{\Gamma(\gamma/2 - iv)\Gamma(\gamma/2+iv)}{\Gamma(\gamma)}\,.$$

The integrand is

$$\frac{e^{iuv}\Gamma(\gamma/2 - iv)\Gamma(\gamma/2+iv)}{2\pi\cdot B\cdot\Gamma(\gamma)\cdot(v-\lambda_1 i)(v-\lambda_2 i)}\,, \tag{45}$$

which has poles in the upper half-plane at $\lambda_1 i$ and at points v such that $\gamma/2 + iv = -n$ for integers $n \geq 0$, since the Γ-function has poles at the negative integers and zero. In other words, the integrand has poles at $\lambda_1 i$ and at $(n+\gamma/2)i$ for $n \geq 0$.

We can calculate the residue of (45) at $v = \lambda_1 i$ directly, using the fact that if $f(z) = g(z)/h(z)$ has a pole at a, and $g(a) \neq 0$, $h(a) = 0$, and $h'(a) \neq 0$, then

$$\operatorname{Res}\{f(z); a\} = \frac{g(a)}{h'(a)}\,.$$

The residue at $\lambda_1 i$ is therefore

$$\frac{e^{-\lambda_1 u}\Gamma(\gamma/2+\lambda_1)\Gamma(\gamma/2-\lambda_1)}{2\pi i\cdot B\cdot\Gamma(\gamma)\cdot(\lambda_1-\lambda_2)}\,. \tag{46}$$

$\Gamma(z)$ has residue $(-1)^n/n!$ at $z = -n$. (See, for example, Andrews, Askey and Roy (1999, p. 7).) Using this fact, it follows that the residue of (45) at $v = (n+\gamma/2)i$ for integers $n \geq 0$ is

$$\frac{-e^{-u(n+\gamma/2)} \cdot \Gamma(\gamma+n) \cdot \frac{(-1)^n}{n!}}{2\pi i \cdot B \cdot \Gamma(\gamma) \cdot (n+\gamma/2-\lambda_1)(n+\gamma/2-\lambda_2)} \tag{47}$$

Substituting (46) and (47) into (43), we find

$$I = \frac{e^{-\lambda_1 u}\Gamma(\gamma/2+\lambda_1)\Gamma(\gamma/2-\lambda_1)}{B \cdot \Gamma(\gamma) \cdot (\lambda_1-\lambda_2)} - e^{-\gamma u/2} \sum_{n=0}^{\infty} \frac{(-e^{-u})^n \cdot \Gamma(\gamma+n) \cdot \frac{1}{n!}}{B \cdot \Gamma(\gamma) \cdot (n+\gamma/2-\lambda_1)(n+\gamma/2-\lambda_2)}$$

Since $|-e^{-u}| < 1$ under the assumption that $u > 0$, which for the time being is still maintained, we can use the series definition of Gauss's hypergeometric function (13), together with the fact that $\Gamma(\gamma+n)/\Gamma(\gamma) = \gamma(\gamma+1)\cdots(\gamma+n-1)$, to obtain

$$\begin{aligned} I &= \frac{e^{-\lambda_1 u}}{B(\lambda_1-\lambda_2)} \frac{\Gamma(\gamma/2-\lambda_1)\Gamma(\gamma/2+\lambda_1)}{\Gamma(\gamma)} + \\ &\quad + \frac{e^{-\gamma u/2}}{B(\lambda_1-\lambda_2)} \left[\frac{1}{\gamma/2-\lambda_2} F\left(\gamma, \gamma/2-\lambda_2; 1+\gamma/2-\lambda_2; -e^{-u}\right) - \right. \\ &\quad \left. - \frac{1}{\gamma/2-\lambda_1} F\left(\gamma, \gamma/2-\lambda_1; 1+\gamma/2-\lambda_1; -e^{-u}\right) \right] \end{aligned} \tag{48}$$

Step 3. A final simplification follows from the fact that

$$\begin{aligned} e^{-\lambda_1 u} \frac{\Gamma(\gamma/2-\lambda_1)\Gamma(\gamma/2+\lambda_1)}{\Gamma(\gamma)} &= \frac{e^{\gamma u/2}}{\gamma/2+\lambda_1} F\left(\gamma, \gamma/2+\lambda_1; 1+\gamma/2+\lambda_1; -e^{u}\right) + \\ &\quad + \frac{e^{-\gamma u/2}}{\gamma/2-\lambda_1} F\left(\gamma, \gamma/2-\lambda_1; 1+\gamma/2-\lambda_1; -e^{-u}\right), \end{aligned}$$

which follows from equation (1.8.1.11) of Slater (1966, pp. 35–36).

Using this observation to substitute out the first term in (48), we have

$$\begin{aligned} I &= \frac{1}{B(\lambda_1-\lambda_2)} \left[\frac{e^{\gamma u/2}}{\gamma/2+\lambda_1} F\left(\gamma, \gamma/2+\lambda_1; 1+\gamma/2+\lambda_1; -e^{u}\right) + \right. \\ &\quad \left. + \frac{e^{-\gamma u/2}}{\gamma/2-\lambda_2} F\left(\gamma, \gamma/2-\lambda_2; 1+\gamma/2-\lambda_2; -e^{-u}\right) \right]. \end{aligned}$$

Substituting this expression into (41) gives the formula

$$\begin{aligned} P/D_1(u) &= \frac{[2\cosh(u/2)]^\gamma}{B(\lambda_1-\lambda_2)} \left[\frac{e^{\gamma u/2}}{\gamma/2+\lambda_1} F\left(\gamma, \gamma/2+\lambda_1; 1+\gamma/2+\lambda_1; -e^{u}\right) + \right. \\ &\quad \left. + \frac{e^{-\gamma u/2}}{\gamma/2-\lambda_2} F\left(\gamma, \gamma/2-\lambda_2; 1+\gamma/2-\lambda_2; -e^{-u}\right) \right]; \end{aligned} \tag{49}$$

thus far, however, the derivation is valid only under the assumption that $u > 0$.

Step 4. Suppose, now, that $u < 0$. Take the complex conjugate of equation (40). (This leaves the left-hand side unaltered because the price-dividend ratio is real.) Doing so is equivalent to reframing the problem with $(u, \lambda_1, \lambda_2)$ replaced by $(-u, -\lambda_2, -\lambda_1)$. Since $-u > 0$, $-\lambda_2 > 0$, and $-\lambda_1 < 0$, the method of steps 1–4 applies unchanged. Since the formula (49) is invariant under $(-u, -\lambda_2, -\lambda_1) \mapsto (u, \lambda_1, \lambda_2)$, we can conclude that equation (49) is valid for all u. Substituting $u \mapsto \log(1-s)/s$ delivers (14).

Step 5. It only remains to find the values of B, λ_1, and λ_2 in terms of the fundamental parameters. The CGF is

$$\boldsymbol{c}(\theta_1, \theta_2) = \mu_1\theta_1 + \mu_2\theta_2 + \frac{1}{2}\sigma_{11}\theta_1^2 + \sigma_{12}\theta_1\theta_2 + \frac{1}{2}\sigma_{22}\theta_2^2.$$

We can rewrite $\rho - \boldsymbol{c}(\alpha_1 - \gamma/2 - iv, \alpha_2 - \gamma/2 + iv)$ in the form

$$\rho - \boldsymbol{c}(\alpha_1 - \gamma/2 - iv, \alpha_2 - \gamma/2 + iv) = \frac{1}{2}X^2v^2 + iYv + \frac{1}{2}Z^2\,, \tag{50}$$

where, as in the main text, I have defined

$$\begin{aligned}
X^2 &\equiv \sigma_{11} - 2\sigma_{12} + \sigma_{22} \\
Y &\equiv \mu_1 - \mu_2 + \alpha_1(\sigma_{11} - \sigma_{12}) - \alpha_2(\sigma_{22} - \sigma_{12}) - \frac{\gamma}{2}(\sigma_{11} - \sigma_{22}) \\
Z^2 &\equiv 2(\rho - \alpha_1\mu_1 - \alpha_2\mu_2) - (\alpha_1^2\sigma_{11} + 2\alpha_1\alpha_2\sigma_{12} + \alpha_2^2\sigma_{22}) + \\
&\quad + \gamma\left[\mu_1 + \mu_2 + \alpha_1\sigma_{11} + (\alpha_1 + \alpha_2)\sigma_{12} + \alpha_2\sigma_{22}\right] - \frac{\gamma^2}{4}(\sigma_{11} + 2\sigma_{12} + \sigma_{22})\,.
\end{aligned}$$

I have chosen to write X^2 and Z^2 to emphasize that these two quantities are positive. The positivity of X^2 follows because it is the variance of the difference of two random variables $(y_{21} - y_{11})$. The positivity of Z^2, on the other hand, follows from the finiteness conditions in Table 1, after setting $v = 0$ in (50).

From (50), we have, finally, that

$$\rho - \boldsymbol{c}(\alpha_1 - \gamma/2 - iv, \alpha_2 - \gamma/2 + iv) = B(v - \lambda_1 i)(v - \lambda_2 i)$$

where

$$\begin{aligned}
B &\equiv \frac{1}{2}X^2 \\
\lambda_1 &\equiv \frac{\sqrt{Y^2 + X^2Z^2} - Y}{X^2} \\
\lambda_2 &\equiv -\frac{\sqrt{Y^2 + X^2Z^2} + Y}{X^2}\,.
\end{aligned}$$

D Small asset asymptotics

I start by establishing the claim made in the text that $\rho - \boldsymbol{c}(1-\theta, \theta-\gamma)$ is a concave function of θ. This fact follows directly from

Proposition 12 (A convexity property of $\boldsymbol{c}(\cdot,\cdot)$)**.** *For arbitrary real numbers α and β, the function $\boldsymbol{c}(\alpha-\theta, \beta+\theta)$ is a convex function of θ.*

Proof. Define the measure $\widehat{\mathbb{P}}$ by

$$\widehat{\mathbb{E}}(A) \equiv e^{-\boldsymbol{c}(\alpha,\beta)}\mathbb{E}\left(e^{\alpha y_{11}+\beta y_{21}}A\right).$$

It follows that the CGF of $y_{21}-y_{11}$, calculated with respect to $\widehat{\mathbb{P}}$, is

$$\begin{aligned}
\widehat{\boldsymbol{c}}(\theta) &= \log\widehat{\mathbb{E}}\left(e^{\theta y_{21}-\theta y_{11}}\right) \\
&= -\boldsymbol{c}(\alpha,\beta) + \log\mathbb{E}\left(e^{(\alpha-\theta)y_{11}+(\beta+\theta)y_{21}}\right) \\
&= -\boldsymbol{c}(\alpha,\beta) + \boldsymbol{c}(\alpha-\theta,\beta+\theta).
\end{aligned}$$

Therefore, $\boldsymbol{c}(\alpha-\theta,\beta+\theta) = \boldsymbol{c}(\alpha,\beta) + \widehat{\boldsymbol{c}}(\theta)$. (Compare also equations (24) and (25) of Appendix A.1.1.)

The convexity of $\boldsymbol{c}(\alpha-\theta,\beta+\theta)$ follows immediately, because $\widehat{\boldsymbol{c}}(\theta)$, as a CGF, is convex, as shown in Billingsley (1995, pp. 147–8). □

The price-dividend ratio in the small asset limit is given by (6), which can be rewritten

$$P/D_1 = \lim_{u\to\infty} \frac{\displaystyle\int_{-\infty}^{\infty} \frac{e^{iuv}\mathscr{F}_\gamma(v)}{\rho - \boldsymbol{c}(1-\gamma/2-iv, -\gamma/2+iv)}\,dv}{\displaystyle\int_{-\infty}^{\infty} e^{iuv}\mathscr{F}_\gamma(v)\,dv}. \tag{51}$$

By the Riemann-Lebesgue lemma, both the numerator and denominator on the right-hand side of (51) tend to zero in the limit as u tends to infinity. What happens to their ratio? This section shows how to calculate limiting price-dividend ratio, riskless rate and excess returns in the small-asset case. For clarity, I work through the price-dividend ratio in detail; the techniques used also apply to the riskless rate and to expected returns.

The following definition provides a convenient label for the poles that will be of interest when evaluating the relevant integrals in the asymptotic limit. (By the finiteness condition and Proposition 10 of Appendix B, the functions to which the definition will be applied will never have poles *on* the real axis.)

Definition 3. *Let f be an arbitrary meromorphic function. A pole (resp. zero) of f is* minimal *if it lies in the upper half-plane and no other pole (resp. zero) in the upper half-plane has smaller imaginary part.*

Step 1. Consider the integral which makes up the numerator of (51),

$$I \equiv \int_{-\infty}^{\infty} \frac{e^{iuv}\mathscr{F}_\gamma(v)}{\rho - \boldsymbol{c}(1-\gamma/2-iv, -\gamma/2+iv)}\, dv\,.$$

If log dividends are drifting Brownian motions, Appendix C showed that this integral could be approached by summing all residues in the upper half-plane. The aim here is to show that the *asymptotic* behavior of this integral is determined only by the minimal residue. Roughly speaking, this is because poles with larger imaginary parts are rendered asymptotically irrelevant by the term e^{iuv}.

To establish this fact, it is convenient to integrate around a contour which avoids all poles except for the minimal pole. If the minimal pole occurs at the minimal zero of $\rho - \boldsymbol{c}(1-\gamma/2-iv, -\gamma/2+iv)$ then, by Proposition 11 of Appendix B, this pole occurs on the imaginary axis. Otherwise, the minimal pole occurs at the minimal pole of $\mathscr{F}_\gamma(v)$, so is at $i\gamma/2$—which is also on the imaginary axis. In short, we can assume that the minimal pole occurs at the point mi, where $m > 0$ is a real number.

Let $\square_N$ denote the rectangle in the complex plane with corners at $-N$, N, $N + (m+\varepsilon)i$ and $-N+(m+\varepsilon)i$, with the understanding that integration will take place in the anticlockwise direction. Since the integrand is meromorphic, all poles are isolated, so $\varepsilon > 0$ can be chosen to be sufficiently small that the rectangle $\square_N$ only contains the pole at mi.

By the residue theorem, we have

$$\begin{aligned} J &\equiv \int_{\square_N} \frac{e^{iuv}\mathscr{F}_\gamma(v)}{\rho - \boldsymbol{c}(1-\gamma/2-iv, -\gamma/2+iv)}\, dv \\ &= 2\pi i \,\mathrm{Res}\left\{ \frac{e^{iuv}\mathscr{F}_\gamma(v)}{\rho - \boldsymbol{c}(1-\gamma/2-iv, -\gamma/2+iv)}; mi \right\} \end{aligned}$$

On the other hand, we can also decompose the integral into four pieces:

$$\begin{aligned} J &= \int_{-N}^{N} \frac{e^{iuv}\mathscr{F}_\gamma(v)}{\rho - \boldsymbol{c}(1-\gamma/2-iv, -\gamma/2+iv)}\, dv + \int_0^{m+\varepsilon} \frac{e^{iu(N+iv)}\mathscr{F}_\gamma(N+iv)}{\rho - \boldsymbol{c}(\ldots)}\, i\, dv + \\ &\quad + \int_N^{-N} \frac{e^{iu(v+(m+\varepsilon)i)}\mathscr{F}_\gamma(v+(m+\varepsilon)i)}{\rho - \boldsymbol{c}(\ldots)}\, dv + \int_{m+\varepsilon}^{0} \frac{e^{iu(-N+iv)}\mathscr{F}_\gamma(-N+iv)}{\rho - \boldsymbol{c}(\ldots)}\, i\, dv \\ &\equiv J_1 + J_2 + J_3 + J_4 \end{aligned}$$

In brief, the desired result follows on first letting N tend to infinity; then J_2 and J_4 go to zero. Subsequently letting u go to infinity, J_3 becomes asymptotically irrelevant compared to J_1. By the residue theorem, the integral $I = \lim_{N\to\infty} J_1$ is therefore asymptotically equivalent[15] to $2\pi i$ times the residue at mi:

$$I \sim 2\pi i \cdot \text{Res}\left\{\frac{e^{iuv}\mathscr{F}_\gamma(v)}{\rho - \boldsymbol{c}(1-\gamma/2-iv, -\gamma/2+iv)}; mi\right\}.$$

The following calculations justify these statements. Consider J_2. Since the range of integration is a closed and bounded interval, the function $|\rho - \boldsymbol{c}(\ldots)|$ attains its maximum and minimum on the range. Since the function has no zeros on the interval, we can write $|\rho - \boldsymbol{c}(\ldots)| \geq \delta_1 > 0$ for all v in the range of integration. We have

$$\begin{aligned}
|J_2| &\leq \int_0^{m+\varepsilon} \left|\frac{e^{iu(N+iv)}\mathscr{F}_\gamma(N+iv)}{\rho - \boldsymbol{c}(\ldots)} i\right| dv \\
&= \int_0^{m+\varepsilon} \frac{e^{-uv}\,|\mathscr{F}_\gamma(N+iv)|}{|\rho - \boldsymbol{c}(\ldots)|} dv \\
&\leq \frac{1}{\delta_1}\int_0^{m+\varepsilon} |\mathscr{F}_\gamma(N+iv)|\, dv \\
&\to 0
\end{aligned}$$

as N tends to infinity because $|\mathscr{F}_\gamma(N+iv)|$ converges to zero uniformly over v in the range of integration. An almost identical argument shows that $|J_4|$ tends to zero as N tends to infinity.

Now consider J_3. Set $\delta_2 = |\rho - \boldsymbol{c}(1-\gamma/2+m+\varepsilon, -\gamma/2-m-\varepsilon)| > 0$; then by the ridge property discussed in Appendix B, $|\rho - \boldsymbol{c}(\ldots)| \geq \delta_2$ for all v in the range of integration. It follows that

$$\begin{aligned}
|J_3| &\leq \int_{-N}^{N} \frac{e^{-(m+\varepsilon)u}\,|\mathscr{F}_\gamma(v+(m+\varepsilon)i)|}{|\rho - \boldsymbol{c}(\ldots)|} dv \\
&\leq e^{-u(m+\varepsilon)} \cdot \frac{1}{\delta_2}\int_{-N}^{N} |\mathscr{F}_\gamma(v+(m+\varepsilon)i)|\, dv \\
&\to e^{-u(m+\varepsilon)} \cdot X/\delta_2
\end{aligned}$$

where X is the (finite) limit of the integral $\int_{-N}^{N} |\mathscr{F}_\gamma(v+(m+\varepsilon)i)|\, dv$ as N tends to infinity. (X is finite because $\mathscr{F}_\gamma(v+(m+\varepsilon)i)$ decays to zero exponentially fast as $v \to \pm\infty$.)

[15] I write $f(x) \sim g(x)$ if $\lim_{x\to\infty} f(x)/g(x) = 1$, and $f(x) = O(g(x))$ if $\lim_{x\to\infty} f(x)/g(x)$ is finite.

By the residue theorem,

$$J_1 + J_2 + J_3 + J_4 = 2\pi i \times \text{residue at } mi = O(e^{-mu})\,.$$

Let N go to infinity; then J_2 and J_4 go to zero, J_1 tends to I and J_3 tends to $e^{-u(m+\varepsilon)}X$, so

$$I + e^{-u(m+\varepsilon)}X = 2\pi i \times \text{residue at } mi = O(e^{-mu})\,.$$

In the limit as $u \to \infty$, $e^{-u(m+\varepsilon)}X$ is exponentially smaller than e^{-mu}, so

$$I \sim 2\pi i \,\mathrm{Res}\left\{\frac{e^{iuv}\mathscr{F}_\gamma(v)}{\rho - \boldsymbol{c}(1-\gamma/2-iv, -\gamma/2+iv)}; mi\right\}$$

as $u \to \infty$. The asymptotic behavior of the integral I is dictated by the residue closest to the real line.

Essentially identical arguments can be made to show that the other relevant integrals are asymptotically equivalent to $2\pi i$ times the minimal residue of the relevant integrand; they are omitted to prevent an already complicated argument becoming totally unreadable.

Step 2. I now apply the logic of step 1 to (i) the price-dividend ratio, (ii) the riskless rate and (iii) expected returns.

(i) In the price-dividend ratio case, we have to evaluate

$$\lim_{u\to\infty} P/D(u) = \lim_{u\to\infty} \frac{\displaystyle\int_{-\infty}^{\infty} \frac{e^{iuv}\mathscr{F}_\gamma(v)}{\rho - \boldsymbol{c}(1-\gamma/2-iv, -\gamma/2+iv)}\,dv}{\displaystyle\int_{-\infty}^{\infty} e^{iuv}\mathscr{F}_\gamma(v)\,dv} \equiv \lim_{u\to\infty} \frac{I_n}{I_d}\,. \tag{52}$$

We have just seen that I_n and I_d are asymptotically equivalent to $2\pi i$ times the residue at the pole (of the relevant integrand) with smallest imaginary part. Here, I take this fact as given and refer to the pole (or zero) with least positive imaginary part as the *minimal* pole (or zero).

Consider, then, the more complicated integral I_n. The integrand has a pole at $i\gamma/2$ due to a singularity in $\mathscr{F}_\gamma(v)$. The question is whether or not there is a zero of $\rho - \boldsymbol{c}(1-\gamma/2-iv, -\gamma/2+iv)$ for some v with imaginary part smaller than $\gamma/2$. If there is, then this is the minimal pole. If not, then $i\gamma/2$ is the minimal pole.

In Appendix B, it was shown that the minimal zero of $\rho - \boldsymbol{c}(1-\gamma/2-iv, -\gamma/2+iv)$ lies on the imaginary axis. Thus the zero in question is of the form $z^* i$ for some positive real z^* satisfying $\rho - \boldsymbol{c}(1-\gamma/2+z^*, -\gamma/2-z^*) = 0$. If $z^* < \gamma/2$, we are in the supercritical case; if $z^* > \gamma/2$, we are in the subcritical case.

In the subcritical case, the minimal pole for both integrals is at $i\gamma/2$. We therefore have, asymptotically,

$$\begin{aligned} P/D &\longrightarrow \frac{\operatorname{Res}\left\{\dfrac{e^{iuv}\mathscr{F}_\gamma(v)}{\rho - \boldsymbol{c}(1-\gamma/2-iv, -\gamma/2+iv)}; i\gamma/2\right\}}{\operatorname{Res}\left\{e^{iuv}\mathscr{F}_\gamma(v); i\gamma/2\right\}} \\ &= \frac{1}{\rho - \boldsymbol{c}(1,-\gamma)} \cdot \frac{\operatorname{Res}\left\{e^{iuv}\mathscr{F}_\gamma(v); i\gamma/2\right\}}{\operatorname{Res}\left\{e^{iuv}\mathscr{F}_\gamma(v); i\gamma/2\right\}} \\ &= \frac{1}{\rho - \boldsymbol{c}(1,-\gamma)} \end{aligned}$$

In the supercritical case, the minimal pole is at iz^* for I_n and at $i\gamma/2$ for I_d, so

$$\begin{aligned} P/D &\longrightarrow \frac{\operatorname{Res}\left\{\dfrac{e^{iuv}\mathscr{F}_\gamma(v)}{\rho - \boldsymbol{c}(1-\gamma/2-iv, -\gamma/2+iv)}; iz^*\right\}}{\operatorname{Res}\left\{e^{iuv}\mathscr{F}_\gamma(v); i\gamma/2\right\}} \\ &= e^{u(\gamma/2-z^*)} \cdot \frac{\operatorname{Res}\left\{\dfrac{\mathscr{F}_\gamma(v)}{\rho - \boldsymbol{c}(1-\gamma/2-iv, -\gamma/2+iv)}; iz^*\right\}}{\operatorname{Res}\left\{\mathscr{F}_\gamma(v); i\gamma/2\right\}} \\ &\longrightarrow \infty \end{aligned}$$

as u tends to infinity because $\gamma/2 - z^* > 0$.

To see that the price-consumption ratio, $P/C = s \cdot P/D$, remains finite in this limit, we must evaluate $\lim_{s\to 0} s \cdot P/D$. Since $s = 1/(1+e^u) \sim e^{-u}$, we have, asymptotically,

$$P/C \longrightarrow e^{u(\gamma/2-z^*-1)} \cdot \frac{\operatorname{Res}\left\{\dfrac{\mathscr{F}_\gamma(v)}{\rho - \boldsymbol{c}(1-\gamma/2-iv, -\gamma/2+iv)}; iz^*\right\}}{\operatorname{Res}\left\{\mathscr{F}_\gamma(v); i\gamma/2\right\}},$$

which tends to zero as $u \to \infty$ because $\gamma/2 - z^* - 1 < 0$.

(ii) In the riskless rate case, we seek the limit of

$$r = \frac{\displaystyle\int_{-\infty}^{\infty} \mathscr{F}_\gamma(v) e^{iuv} \cdot [\rho - \boldsymbol{c}(-\gamma/2-iv, -\gamma/2+iv)]\, dv}{\displaystyle\int_{-\infty}^{\infty} \mathscr{F}_\gamma(v) e^{iuv}\, dv}.$$

This is much simpler, because the minimal pole is $i\gamma/2$ for both numerator and denominator. It follows that

$$r \longrightarrow \rho - \boldsymbol{c}(-\gamma/2 - i(i\gamma/2), -\gamma/2 + i(i\gamma/2)) = \rho - \boldsymbol{c}(0,-\gamma).$$

(iii) In the expected return case, we need the limit of the expected capital gain expression which is the first term on the right-hand side of (9). This expression is asymptotically equivalent to

$$\frac{\displaystyle\int_{-\infty}^{\infty} \frac{e^{iuv}\mathscr{F}_\gamma(v)\boldsymbol{c}(1-\gamma/2-iv,\gamma/2+iv)}{\rho-\boldsymbol{c}(1-\gamma/2-iv,-\gamma/2+iv)}\,dv}{\displaystyle\int_{-\infty}^{\infty} \frac{e^{iuv}\mathscr{F}_\gamma(v)}{\rho-\boldsymbol{c}(1-\gamma/2-iv,-\gamma/2+iv)}\,dv} \equiv \frac{J_n}{J_d}$$

since the higher-order exponential terms e^{-mu} for $m \geq 1$ which appear in (9) become irrelevant exponentially fast as u tends to infinity. Again, there are two subcases, depending on whether the minimal zero of $\rho-\boldsymbol{c}(1-\gamma/2-iv,-\gamma/2+iv)$ has imaginary part greater than or less than $\gamma/2$.

In the subcritical case, the minimal pole of each of J_n and J_d occurs at $i\gamma/2$, so

$$\begin{aligned}\lim_{u\to\infty} \mathbb{E}dP/P &= \frac{\operatorname{Res}\left\{\dfrac{e^{iuv}\mathscr{F}_\gamma(v)\boldsymbol{c}(1-\gamma/2-iv,\gamma/2+iv)}{\rho-\boldsymbol{c}(1-\gamma/2-iv,-\gamma/2+iv)}; i\gamma/2\right\}}{\operatorname{Res}\left\{\dfrac{e^{iuv}\mathscr{F}_\gamma(v)}{\rho-\boldsymbol{c}(1-\gamma/2-iv,-\gamma/2+iv)}; i\gamma/2\right\}} \\ &= \boldsymbol{c}(1,0)\,.\end{aligned}$$

In the supercritical case, the minimal pole of each of J_n and J_d occurs at iz^*, so

$$\begin{aligned}\lim_{u\to\infty} \mathbb{E}dP/P &= \frac{\operatorname{Res}\left\{\dfrac{e^{iuv}\mathscr{F}_\gamma(v)\boldsymbol{c}(1-\gamma/2-iv,\gamma/2+iv)}{\rho-\boldsymbol{c}(1-\gamma/2-iv,-\gamma/2+iv)}; iz^*\right\}}{\operatorname{Res}\left\{\dfrac{e^{iuv}\mathscr{F}_\gamma(v)}{\rho-\boldsymbol{c}(1-\gamma/2-iv,-\gamma/2+iv)}; iz^*\right\}} \\ &= \boldsymbol{c}(1-\gamma/2+z^*,\gamma/2-z^*)\,.\end{aligned}$$

Since instantaneous expected returns are the sum of expected capital gains and the dividend-price ratio, expected returns in the asymptotic limit are $\boldsymbol{c}(1,0)+\rho-\boldsymbol{c}(1,-\gamma)$ in the subcritical case, and $\boldsymbol{c}(1-\gamma/2+z^*,\gamma/2-z^*)$ in the supercritical case.

Subtracting the riskless rate, we have, finally, that excess returns are $\boldsymbol{c}(1,0)+\boldsymbol{c}(0,-\gamma)-\boldsymbol{c}(1,-\gamma)$ in the subcritical case, and $\boldsymbol{c}(1-\gamma/2+z^*,\gamma/2-z^*)-\rho+\boldsymbol{c}(0,-\gamma)$ in the supercritical case. Recalling that $\rho=\boldsymbol{c}(1-\gamma/2+z^*,-\gamma/2-z^*)$ by the definition of z^*, the excess return in the supercritical case can be rewritten as

$$\boldsymbol{c}(1-\gamma/2+z^*,\gamma/2-z^*)+\boldsymbol{c}(0,-\gamma)-\boldsymbol{c}(1-\gamma/2+z^*,-\gamma/2-z^*)\,.$$

Step 3. If dividends are also independent across assets then we can decompose $\boldsymbol{c}(\theta_1, \theta_2) = \boldsymbol{c}_1(\theta_1) + \boldsymbol{c}_2(\theta_2)$ where $\boldsymbol{c}_i(\theta) \equiv \log \mathbb{E} \exp \theta y_{i1}$. It follows that in the subcritical case,

$$XS \longrightarrow \boldsymbol{c}(1,0) + \boldsymbol{c}(0,-\gamma) - \boldsymbol{c}(1,-\gamma) = 0$$

and in the supercritical case,

$$\begin{aligned} XS &\longrightarrow \boldsymbol{c}(1-\gamma/2+z^*, \gamma/2-z^*) + \boldsymbol{c}(0,-\gamma) - \boldsymbol{c}(1-\gamma/2+z^*, -\gamma/2-z^*) \\ &= \boldsymbol{c}_2(\gamma/2-z^*) + \boldsymbol{c}_2(-\gamma) - \boldsymbol{c}_2(-\gamma/2-z^*)\,. \end{aligned}$$

Step 4. I now show that this last expression is positive. First, note that because $\boldsymbol{c}_2(x)$—as a CGF—is convex, we have that

$$\frac{\boldsymbol{c}_2(e) - \boldsymbol{c}_2(d)}{e-d} < \frac{\boldsymbol{c}_2(g) - \boldsymbol{c}_2(f)}{g-f} \quad \text{whenever } d < e < f < g\,.$$

Next, observe that in the supercritical case, we have $-\gamma < -\gamma/2 - z^* < 0 < \gamma/2 - z^*$. It follows that

$$\frac{\boldsymbol{c}_2(-\gamma/2-z^*) - \boldsymbol{c}_2(-\gamma)}{(-\gamma/2-z^*) - (-\gamma)} < \frac{\boldsymbol{c}_2(\gamma/2-z^*) - \boldsymbol{c}_2(0)}{(\gamma/2-z^*) - 0}\,,$$

or equivalently, because $\boldsymbol{c}_2(0) = 0$, $\boldsymbol{c}_2(-\gamma/2-z^*) - \boldsymbol{c}_2(-\gamma) < \boldsymbol{c}_2(\gamma/2-z^*)$, and so $\boldsymbol{c}_2(\gamma/2-z^*) + \boldsymbol{c}_2(-\gamma) - \boldsymbol{c}_2(-\gamma/2-z^*) > 0$, as required.

Step 5. The last step showed that $R_1 = R_f$ in the subcritical case and $R_1 > R_f$ in the supercritical case. It only remains to show that the other bounds on expected returns hold: that (i) $R_1 < R_2$, assuming independence, and that (ii) in the supercritical case $R_1 < G_1$, assuming $G_1 \geq G_2$.

Step 5(i). Proof that $R_1 < R_2$, assuming independence of dividends:

In the subcritical case, $R_1 = \rho + \boldsymbol{c}(1,0) - \boldsymbol{c}(1,-\gamma)$ and $R_2 = \rho + \boldsymbol{c}(0,1) - \boldsymbol{c}(0,1-\gamma)$. Since we are assuming independence, we must show that $-\boldsymbol{c}_2(-\gamma) < \boldsymbol{c}_2(1) - \boldsymbol{c}_2(1-\gamma)$, or equivalently that $\boldsymbol{c}_2(1-\gamma) < \boldsymbol{c}_2(1) + \boldsymbol{c}_2(-\gamma)$, which follows by convexity of $\boldsymbol{c}_2(\cdot)$.

In the supercritical case, $R_1 = \boldsymbol{c}(1-\gamma/2+z^*, \gamma/2-z^*)$ and $R_2 = \boldsymbol{c}(1-\gamma/2+z^*, -\gamma/2-z^*) + \boldsymbol{c}(0,1) - \boldsymbol{c}(0,1-\gamma)$ (substituting in for ρ from the definition of z^*). By independence, it remains to show that $\boldsymbol{c}_2(\gamma/2-z^*) < \boldsymbol{c}_2(-\gamma/2-z^*) + \boldsymbol{c}_2(1) - \boldsymbol{c}_2(1-\gamma)$, or equivalently that $\boldsymbol{c}_2(1-\gamma) + \boldsymbol{c}_2(\gamma/2-z^*) < \boldsymbol{c}_2(1) + \boldsymbol{c}_2(-\gamma/2-z^*)$, which also follows directly by convexity of $\boldsymbol{c}_2(\cdot)$, since $\gamma/2 - z^* \in (0,1)$.

Step 5(ii). Next, I show that in the supercritical case, $R_1 \leq G_1$ if $G_1 \geq G_2$. We do not need the independence assumption here. It will be helpful to write $\theta =$

$\gamma/2 - z^* \in (0,1)$. With this notation, the limiting $R_1 = \boldsymbol{c}(1-\theta,\theta)$. The claim is that $\boldsymbol{c}(1-\theta,\theta) \leq \boldsymbol{c}(1,0)$. To show this, we make the same change of measure as was used in the proof of Proposition 12. We have $R_1 = \boldsymbol{c}(1-\theta,\theta) = \boldsymbol{c}(1,0) + \widehat{\boldsymbol{c}}(-\theta)$. It suffices to show that $\widehat{\boldsymbol{c}}(-\theta) \leq 0$ for all θ in $(0,1)$. We have $\boldsymbol{c}(0,1) = \boldsymbol{c}(1,0) + \widehat{\boldsymbol{c}}(-1)$, and so by assumption $\widehat{\boldsymbol{c}}(-1) \leq 0$. Since $\widehat{\boldsymbol{c}}(0) = 0$, the claim follows by convexity of $\widehat{\boldsymbol{c}}(\cdot)$.

D.1 Asymptotics near the small-asset limit

To prove Proposition 7, we need to consider the *two* closest residues to the real axis. By assumption $z^* \in (\gamma/2, \gamma/2+1)$, so for price-dividend ratio and excess-return calculations, the closest residue is at $(\gamma/2)i$ and the next closest is at $z^* i$. For the riskless rate calculation, the two closest residues are at $(\gamma/2)i$ and $(\gamma/2+1)i$. The residues at $(\gamma/2)i$ were calculated in the previous section, so proving the proposition is an exercise in computing residues at $z^* i$ and at $(\gamma/2+1)i$ for the integrands in question.

I first carry out the price-dividend ratio calculations. In the numerator of (52), the residue at $z^* i$ is

$$\frac{1}{2\pi i} \cdot \frac{\mathscr{B}(\gamma/2 - z^*, \gamma/2 + z^*)}{\boldsymbol{c}_1(1-\gamma/2+z^*, -\gamma/2-z^*) - \boldsymbol{c}_2(1-\gamma/2+z^*, -\gamma/2-z^*)} \cdot e^{-z^* u}$$

where $\mathscr{B}(x,y) \equiv \Gamma(x)\Gamma(y)/\Gamma(x+y)$ is the beta function and, for example, $\boldsymbol{c}_1(\cdot,\cdot)$ indicates the partial derivative of $\boldsymbol{c}(\cdot,\cdot)$ with respect to its first argument.

In the denominator, the next closest residue to the real axis is at $(\gamma/2+1)i$, and the residue there is

$$\frac{-\gamma}{2\pi i} \cdot e^{-(\gamma/2+1)u}$$

Applying the residue theorem, we have

$$P/D_1 \doteq \frac{\dfrac{e^{-\gamma u/2}}{\rho - \boldsymbol{c}(1,-\gamma)} + \dfrac{e^{-z^* u}\mathscr{B}(\gamma/2 - z^*, \gamma/2 + z^*)}{\boldsymbol{c}_1(1-\gamma/2+z^*, -\gamma/2-z^*) - \boldsymbol{c}_2(1-\gamma/2+z^*, -\gamma/2-z^*)}}{e^{-\gamma u/2} - \gamma e^{-(\gamma/2+1)u}}$$

which after simplification gives

$$P/D_1 \doteq \frac{1}{\rho - \boldsymbol{c}(1,-\gamma)} + \frac{\mathscr{B}(\gamma/2 - z^*, \gamma/2 + z^*)}{\boldsymbol{c}_1(1-\gamma/2+z^*, -\gamma/2-z^*) - \boldsymbol{c}_2(1-\gamma/2+z^*, -\gamma/2-z^*)} \cdot s^{z^* - \gamma/2}$$

using the fact that $e^{-u} \sim s$. So,

$$\begin{aligned}
C &= \frac{1}{\rho - \boldsymbol{c}(1,-\gamma)} \\
D &= \frac{-\mathscr{B}(\gamma/2 - z^*, \gamma/2 + z^*)}{\boldsymbol{c}_1(1-\gamma/2+z^*, -\gamma/2-z^*) - \boldsymbol{c}_2(1-\gamma/2+z^*, -\gamma/2-z^*)}
\end{aligned}$$

$C > 0$ by assumption (16). To see that $D > 0$, note first that $\mathscr{B}(\gamma/2 - z^*, \gamma/2 + z^*)$ is negative, because it equals $\Gamma(\gamma/2 - z^*)\Gamma(\gamma/2 + z^*)/\Gamma(\gamma)$, and $\Gamma(x)$ is negative for $x \in (-1, 0)$ and positive for $x > 0$. Second, the denominator of D is positive; this follows because it has the opposite sign to the derivative of

$$\rho - \boldsymbol{c}(1 - \gamma/2 + z, -\gamma/2 - z) \tag{53}$$

with respect to z, evaluated at z^*. This derivative in turn is negative because (53) is (i) concave (from Proposition 12), (ii) positive at $z = \gamma/2$ by the subcriticality assumption (16), and (iii) zero at $z = z^*$ by definition of z^*. Thus, $D > 0$.

Similar calculations reveal that A, B, E, and F are given by

$$\begin{aligned}
A &= \rho - \boldsymbol{c}(0, -\gamma) \\
B &= \gamma \left[\boldsymbol{c}(1, -1 - \gamma) - \boldsymbol{c}(0, -\gamma)\right] \\
E &= \boldsymbol{c}(1, 0) + \boldsymbol{c}(0, -\gamma) - \boldsymbol{c}(1, -\gamma) \\
F &= \frac{D}{C}\left[\boldsymbol{c}(1, 0) - \boldsymbol{c}(1, -\gamma) + \boldsymbol{c}(1 - \gamma/2 + z^*, -\gamma/2 - z^*) - \boldsymbol{c}(1 - \gamma/2 + z^*, \gamma/2 - z^*)\right]
\end{aligned}$$

None of these four quantities can be signed in general; for example, the dependence of the riskless rate on s may have either sign, depending on which of the two assets has higher volatility in fundamentals. But if the two assets have independent fundamentals, then $E = 0$ (as in Step 3 of the previous subsection) and $F > 0$ (because the expression inside the square brackets is positive, by an almost identical argument to that presented in Step 4 of the previous subsection; the only difference is that the sign of the inequality is reversed because now $\gamma/2 < z^*$, since we are in the subcritical case).

E The N-tree case

E.1 The Fourier transform $\mathscr{F}_\gamma^N(\boldsymbol{v})$

To make a start, we seek the integral

$$I_N \equiv \int_{\mathbb{R}^{N-1}} \frac{e^{-ix_1 v_1 - ix_2 v_2 - \cdots - ix_{N-1} v_{N-1}}}{\left(e^{x_1/N} + \cdots + e^{x_{N-1}/N} + e^{-(x_1 + x_2 + \ldots + x_{N-1})/N}\right)^\gamma}\, dx_1 \ldots dx_{N-1}.$$

For notational convenience, write $x_N \equiv -x_1 - \cdots - x_{N-1}$—so $\sum_1^N x_i = 0$—and, for $i = 1, \ldots, N$, define

$$t_i = \frac{e^{x_i/N}}{e^{x_1/N} + \cdots + e^{x_N/N}}. \tag{54}$$

Note that the variables t_i range between 0 and 1 (and, by construction, sum to 1) as the variables $\{x_i\}$ range around. Furthermore, we have $e^{x_i} = t_i^N / \prod_{k=1}^N t_k$. Of course, because of the linear dependence $\sum_{k=1}^N t_k = 1$, there are only $N-1$ independent variables and $t_N = 1 - t_1 - \cdots - t_{N-1}$, so we can rewrite

$$x_i = N \log t_i - \sum_{k=1}^{N-1} \log t_k - \log\left(1 - \sum_{k=1}^{N-1} t_k\right), \quad i = 1, \ldots, N-1. \tag{55}$$

To make the change of variables specified in (54), we have to calculate the Jacobian

$$J \equiv \left| \frac{\partial(x_1, \ldots, x_{N-1})}{\partial(t_1, \ldots, t_{N-1})} \right| .$$

From (55),

$$\frac{\partial x_i}{\partial t_j} = \frac{1}{t_N} - \frac{1}{t_j} + \frac{N\delta_{ij}}{t_i},$$

where δ_{ij} equals one if $i = j$ and zero otherwise, so

$$\begin{aligned} \frac{\partial(x_1, \ldots, x_{N-1})}{\partial(t_1, \ldots, t_{N-1})} &= \begin{pmatrix} \frac{N}{t_1} & & & \\ & \frac{N}{t_2} & & \\ & & \ddots & \\ & & & \frac{N}{t_{N-1}} \end{pmatrix} + \begin{pmatrix} 1 \\ 1 \\ \vdots \\ 1 \end{pmatrix} \begin{pmatrix} \frac{1}{t_N} - \frac{1}{t_1} \\ \frac{1}{t_N} - \frac{1}{t_2} \\ \vdots \\ \frac{1}{t_N} - \frac{1}{t_{N-1}} \end{pmatrix}' \\ &\equiv \boldsymbol{A} + \boldsymbol{\alpha}\boldsymbol{\beta}'. \end{aligned}$$

The last line defines the $(N-1) \times (N-1)$ matrix $\boldsymbol{A}$ and the $(N-1)$-dimensional column vectors $\boldsymbol{\alpha}$ and $\boldsymbol{\beta}$. $\boldsymbol{A}$ is a diagonal matrix: blanks indicate zeros. The prime symbol ($'$) denotes a transpose.

In order to calculate $J = \det(\boldsymbol{A} + \boldsymbol{\alpha}\boldsymbol{\beta}')$ we can use the following

Fact 1 (Matrix determinant lemma)**.** *Suppose that $\boldsymbol{A}$ is an invertible square matrix and that $\boldsymbol{\alpha}$ and $\boldsymbol{\beta}$ are column vectors, each of length equal to the dimension of $\boldsymbol{A}$. Then*

$$\det(\boldsymbol{A} + \boldsymbol{\alpha}\boldsymbol{\beta}') = \left(1 + \boldsymbol{\beta}'\boldsymbol{A}^{-1}\boldsymbol{\alpha}\right) \det \boldsymbol{A}.$$

This fact is useful in the present case because $\boldsymbol{A}$ is diagonal, so its inverse and determinant are easily calculated. To be specific, $\det \boldsymbol{A} = N^{N-1}/(t_1 \cdots t_{N-1})$, and

$$\boldsymbol{A}^{-1} = \begin{pmatrix} \frac{t_1}{N} & & & \\ & \frac{t_2}{N} & & \\ & & \ddots & \\ & & & \frac{t_{N-1}}{N} \end{pmatrix}.$$

It follows that $J = N^{N-2}/(t_1 \cdots t_N)$.

We can now return to the integral I_N. For typographical reasons, I write Π for the product $\prod_{k=1}^{N} t_k$ and suppress the range of integration, which is $[0,1]^{N-1}$. Making the substitution suggested in (54),

$$\begin{aligned}
I_N &= \int \frac{\left(\frac{t_1^N}{\Pi}\right)^{-iv_1} \left(\frac{t_2^N}{\Pi}\right)^{-iv_2} \cdots \left(\frac{t_{N-1}^N}{\Pi}\right)^{-iv_{N-1}}}{\left(\frac{t_1+t_2+\cdots+t_N}{\Pi^{1/N}}\right)^{\gamma}} \cdot J\, dt_1 \ldots dt_{N-1} \\
&= N^{N-2} \int \Pi^{\gamma/N} \left(\frac{t_1^N}{\Pi}\right)^{-iv_1} \cdots \left(\frac{t_{N-1}^N}{\Pi}\right)^{-iv_{N-1}} \frac{dt_1 \ldots dt_{N-1}}{t_1 \ldots t_{N-1} t_N} \\
&= N^{N-2} \int \Big(t_1^{\gamma/N + iv_1 + \cdots + iv_{N-1} - Niv_1} t_2^{\gamma/N + iv_1 + \cdots + iv_{N-1} - Niv_2} \cdots \\
&\qquad\qquad \cdots t_{N-1}^{\gamma/N + iv_1 + \cdots + iv_{N-1} - Niv_{N-1}} \cdot t_N^{\gamma/N + iv_1 + \cdots + iv_{N-1}} \Big) \frac{dt_1 \ldots dt_{N-1}}{t_1 \ldots t_{N-1} t_N} .
\end{aligned}$$

As in the two-asset case, this is a Dirichlet surface integral. As shown in Andrews, Askey and Roy (1999, p. 34), it can be evaluated in terms of Γ-functions: we have

$$I_N = \frac{N^{N-2}}{\Gamma(\gamma)} \cdot \Gamma\left(\gamma/N + iv_1 + iv_2 + \ldots + iv_{N-1}\right) \cdot \prod_{k=1}^{N-1} \Gamma\left(\gamma/N + iv_1 + \cdots + iv_{N-1} - Niv_k\right) .$$

Defining $\mathscr{G}_\gamma^N(\boldsymbol{v}) = I_N/(2\pi)^{N-1}$, where $\boldsymbol{v} = (v_1, \ldots, v_{N-1})$, we have

$$\mathscr{G}_\gamma^N(\boldsymbol{v}) = \frac{N^{N-2}}{(2\pi)^{N-1}} \cdot \frac{\Gamma\left(\gamma/N + iv_1 + iv_2 + \ldots + iv_{N-1}\right)}{\Gamma(\gamma)} \cdot \prod_{k=1}^{N-1} \Gamma\left(\gamma/N + iv_1 + \cdots + iv_{N-1} - Niv_k\right) . \tag{56}$$

It follows from this definition of $\mathscr{G}_\gamma^N(\boldsymbol{v})$, by the Fourier inversion theorem, that

$$\frac{1}{\left(e^{x_1/N} + e^{x_2/N} + \ldots + e^{-(x_1+x_2+\ldots+x_{N-1})/N}\right)^{\gamma}} = \int_{\mathbb{R}^{N-1}} \mathscr{G}_\gamma^N(\boldsymbol{v}) e^{i\boldsymbol{v}'\boldsymbol{x}}\, d\boldsymbol{v} , \tag{57}$$

where $\boldsymbol{x} = (x_1, \ldots, x_{N-1})$.

E.2 The expectation

We seek the expectation

$$E = \mathbb{E}\left[\frac{e^{\boldsymbol{\alpha}'\widetilde{\boldsymbol{y}}_t}}{\left(e^{y_{10}+\widetilde{y}_{1t}} + \cdots + e^{y_{N0}+\widetilde{y}_{Nt}}\right)^{\gamma}}\right] ,$$

where $\boldsymbol{\alpha} \equiv (\alpha_1, \ldots, \alpha_N)'$ and $\widetilde{\boldsymbol{y}}_t \equiv (\widetilde{y}_{1t}, \ldots, \widetilde{y}_{Nt})'$.

The calculation is carried out by applying the same three tricks that were useful in the two-tree case: namely, by putting the denominator in a form amenable to a Fourier transform; then changing measure, to take care of the numerator; and finally applying the Fourier transform.

The calculations below also use the vectors $\boldsymbol{y}_0$ and $\boldsymbol{\gamma}$ defined in the main text. In addition, define the $(N-1)\times N$ matrix $\boldsymbol{Q}$ and vectors $\boldsymbol{q}_i$ by

$$\boldsymbol{Q} \equiv \begin{pmatrix} \boldsymbol{q}_2' \\ \boldsymbol{q}_3' \\ \vdots \\ \boldsymbol{q}_N' \end{pmatrix} \equiv \begin{pmatrix} -1 & N-1 & -1 & \cdots & -1 \\ -1 & -1 & N-1 & \ddots & \vdots \\ \vdots & \vdots & \ddots & \ddots & -1 \\ -1 & -1 & \cdots & -1 & N-1 \end{pmatrix},$$

and let $\boldsymbol{q}_1 \equiv (N-1,\ldots,-1,-1)'$—the "missing" row which does *not* appear as the top row of $\boldsymbol{Q}$. (This definition is only introduced to make certain expressions neater, since $\boldsymbol{q}_1 = -\sum_{k=2}^N \boldsymbol{q}_k$.)

We will also need to make a change of measure at one stage, as in the two asset case. Define $\widetilde{\mathbb{E}}$ by

$$\widetilde{\mathbb{E}}\left[Y\right] \equiv e^{-t\boldsymbol{c}(\boldsymbol{\alpha}-\boldsymbol{\gamma}/N)} \cdot \mathbb{E}\left[e^{(\boldsymbol{\alpha}-\boldsymbol{\gamma}/N)'\widetilde{\boldsymbol{y}}_t} \cdot Y\right] .$$

It follows that

$$\widetilde{\boldsymbol{c}}(\boldsymbol{v}) \equiv \log \widetilde{\mathbb{E}}\left[e^{\widetilde{\boldsymbol{y}}_1'\boldsymbol{v}}\right] = \boldsymbol{c}(\boldsymbol{\alpha}-\boldsymbol{\gamma}/N+\boldsymbol{v}) - \boldsymbol{c}(\boldsymbol{\alpha}-\boldsymbol{\gamma}/N) .$$

Using the new notation,

$$\begin{aligned} E &= \mathbb{E}\left[\frac{e^{\boldsymbol{\alpha}'\widetilde{\boldsymbol{y}}_t}}{\left(e^{y_{10}+\widetilde{y}_{1t}} + \cdots + e^{y_{N0}+\widetilde{y}_{Nt}}\right)^{\gamma}}\right] \\ &= \mathbb{E}\left[\frac{e^{\boldsymbol{\alpha}'\widetilde{\boldsymbol{y}}_t - \boldsymbol{\gamma}'(\boldsymbol{y}_0+\widetilde{\boldsymbol{y}}_t)/N}}{\left(e^{\boldsymbol{q}_1'(\boldsymbol{y}_0+\widetilde{\boldsymbol{y}}_t)/N} + \cdots + e^{\boldsymbol{q}_N'(\boldsymbol{y}_0+\widetilde{\boldsymbol{y}}_t)/N}\right)^{\gamma}}\right] \\ &= e^{-\boldsymbol{\gamma}'\boldsymbol{y}_0/N} e^{\boldsymbol{c}(\boldsymbol{\alpha}-\boldsymbol{\gamma}/N)t}\, \widetilde{\mathbb{E}}\left[\frac{1}{\left(e^{\boldsymbol{q}_1'(\boldsymbol{y}_0+\widetilde{\boldsymbol{y}}_t)/N} + \cdots + e^{\boldsymbol{q}_N'(\boldsymbol{y}_0+\widetilde{\boldsymbol{y}}_t)/N}\right)^{\gamma}}\right] . \end{aligned}$$

Now, $\boldsymbol{Q}(\boldsymbol{y}_0+\widetilde{\boldsymbol{y}}_t)$ plays the role of $\boldsymbol{x}$ in expression (57). It follows that

$$\begin{aligned} E &= e^{-\boldsymbol{\gamma}'\boldsymbol{y}_0/N} e^{\boldsymbol{c}(\boldsymbol{\alpha}-\boldsymbol{\gamma}/N)t}\, \widetilde{\mathbb{E}}\left[\int \mathscr{G}_\gamma^N(\boldsymbol{v}) e^{i\boldsymbol{v}'\boldsymbol{Q}(\boldsymbol{y}_0+\widetilde{\boldsymbol{y}}_t)}\, d\boldsymbol{v}\right] \\ &= e^{-\boldsymbol{\gamma}'\boldsymbol{y}_0/N} e^{\boldsymbol{c}(\boldsymbol{\alpha}-\boldsymbol{\gamma}/N)t} \int \mathscr{G}_\gamma^N(\boldsymbol{v}) e^{i\boldsymbol{v}'\boldsymbol{Q}\boldsymbol{y}_0} e^{\widetilde{\boldsymbol{c}}(i\boldsymbol{Q}'\boldsymbol{v})t}\, d\boldsymbol{v} \\ &= e^{-\boldsymbol{\gamma}'\boldsymbol{y}_0/N} \int \mathscr{G}_\gamma^N(\boldsymbol{v}) e^{i\boldsymbol{v}'\boldsymbol{Q}\boldsymbol{y}_0} e^{\boldsymbol{c}(\boldsymbol{\alpha}-\boldsymbol{\gamma}/N+i\boldsymbol{Q}'\boldsymbol{v})t}\, d\boldsymbol{v} . \end{aligned} \tag{58}$$

E.3 Prices

Now we proceed along the same lines as in the two-tree case.

$$\begin{aligned} P &= \mathbb{E}\int_0^\infty e^{-\rho t}\left(\frac{C_t}{C_0}\right)^{-\gamma} D_{1t}^{\alpha_1}\cdots D_{Nt}^{\alpha_N}\,dt \\ &= C_0^\gamma \int_0^\infty e^{-\rho t}\mathbb{E}\left[\frac{e^{\alpha_1(y_{10}+\widetilde{y}_{1t})+\cdots+\alpha_N(y_{N0}+\widetilde{y}_{Nt})}}{\left(e^{y_{10}+\widetilde{y}_{1t}}+\cdots+e^{y_{N0}+\widetilde{y}_{Nt}}\right)^\gamma}\right] dt\,. \end{aligned}$$

The price-dividend ratio is therefore equal to

$$P/D = C_0^\gamma \int_0^\infty e^{-\rho t}\mathbb{E}\left[\frac{e^{\alpha_1\widetilde{y}_{1t}+\cdots+\alpha_N\widetilde{y}_{Nt}}}{\left(e^{y_{10}+\widetilde{y}_{1t}}+\cdots+e^{y_{N0}+\widetilde{y}_{Nt}}\right)^\gamma}\right] dt\,,$$

and the expectation was calculated in the previous section. Substituting in from (58),

$$\begin{aligned} P/D &= C_0^\gamma \int_{t=0}^\infty e^{-\rho t}\left(e^{-\boldsymbol{\gamma}'\boldsymbol{y}_0/N}\int \mathscr{G}_\gamma^N(\boldsymbol{v})e^{i\boldsymbol{v}'\boldsymbol{Q}\boldsymbol{y}_0}e^{\boldsymbol{c}(\boldsymbol{\alpha}-\boldsymbol{\gamma}/N+i\boldsymbol{Q}'\boldsymbol{v})t}\,d\boldsymbol{v}\right) dt \\ &= C_0^\gamma e^{-\boldsymbol{\gamma}'\boldsymbol{y}_0/N}\int \frac{\mathscr{G}_\gamma^N(\boldsymbol{v})e^{i\boldsymbol{v}'\boldsymbol{Q}\boldsymbol{y}_0}}{\rho-\boldsymbol{c}(\boldsymbol{\alpha}-\boldsymbol{\gamma}/N+i\boldsymbol{Q}'\boldsymbol{v})}\,d\boldsymbol{v} \qquad (59) \\ &= \left(e^{\boldsymbol{q}_1'\boldsymbol{y}_0/N}+\cdots+e^{\boldsymbol{q}_N'\boldsymbol{y}_0/N}\right)^\gamma \int \frac{\mathscr{G}_\gamma^N(\boldsymbol{v})e^{i\boldsymbol{v}'\boldsymbol{Q}\boldsymbol{y}_0}}{\rho-\boldsymbol{c}(\boldsymbol{\alpha}-\boldsymbol{\gamma}/N+i\boldsymbol{Q}'\boldsymbol{v})}\,d\boldsymbol{v}\,. \end{aligned}$$

As in the two-asset case, I assume that $\mathrm{Re}\left[\rho-\boldsymbol{c}(\boldsymbol{\alpha}-\boldsymbol{\gamma}/N+i\boldsymbol{Q}'\boldsymbol{v})\right]>0$; and as in the two-asset case, this follows from the apparently weaker condition that $\rho-\boldsymbol{c}(\boldsymbol{\alpha}-\boldsymbol{\gamma}/N)>0$. The proof follows the same lines as in the two-asset case, so is omitted.

E.4 Returns

From (59), the price of the $\boldsymbol{\alpha}$-asset is

$$P = \left(e^{y_{10}}+\cdots+e^{y_{N0}}\right)^\gamma e^{(\boldsymbol{\alpha}-\boldsymbol{\gamma}/N)'\boldsymbol{y}_0}\int \frac{\mathscr{G}_\gamma^N(\boldsymbol{v})e^{i\boldsymbol{v}'\boldsymbol{Q}\boldsymbol{y}_0}}{\rho-\boldsymbol{c}(\boldsymbol{\alpha}-\boldsymbol{\gamma}/N+i\boldsymbol{Q}'\boldsymbol{v})}\,d\boldsymbol{v}\,.$$

Introducing the *multinomial coefficient*,

$$\binom{\gamma}{\boldsymbol{m}} \equiv \frac{\gamma!}{m_1!m_2!\cdots m_N!}\,,$$

we can express the price as

$$P = \sum_{\boldsymbol{m}}\binom{\gamma}{\boldsymbol{m}}\int \frac{\mathscr{G}_\gamma^N(\boldsymbol{v})e^{(\boldsymbol{\alpha}-\boldsymbol{\gamma}/N+\boldsymbol{m}+i\boldsymbol{Q}'\boldsymbol{v})'\boldsymbol{y}_0}}{\rho-\boldsymbol{c}(\boldsymbol{\alpha}-\boldsymbol{\gamma}/N+i\boldsymbol{Q}'\boldsymbol{v})}\,d\boldsymbol{v}\,.$$

The sum is taken over all N-dimensional vectors $\boldsymbol{m}$ whose entries are nonnegative integers which add up to γ.

Using the result of Appendix A.1.3, it follows that

$$\mathbb{E}dP = \sum_{\boldsymbol{m}} \binom{\gamma}{\boldsymbol{m}} \int \frac{\mathscr{G}_\gamma^N(\boldsymbol{v}) e^{(\boldsymbol{\alpha}-\boldsymbol{\gamma}/N+\boldsymbol{m}+i\boldsymbol{Q}'\boldsymbol{v})'\boldsymbol{y}_0} \boldsymbol{c}(\boldsymbol{\alpha}-\boldsymbol{\gamma}/N+\boldsymbol{m}+i\boldsymbol{Q}'\boldsymbol{v})}{\rho - \boldsymbol{c}(\boldsymbol{\alpha}-\boldsymbol{\gamma}/N+i\boldsymbol{Q}'\boldsymbol{v})}\, d\boldsymbol{v}\, dt\,,$$

and hence

$$\begin{aligned}
\mathbb{E}dP/D &= \sum_{\boldsymbol{m}} \binom{\gamma}{\boldsymbol{m}} \int \frac{\mathscr{G}_\gamma^N(\boldsymbol{v}) e^{(-\boldsymbol{\gamma}/N+\boldsymbol{m}+i\boldsymbol{Q}'\boldsymbol{v})'\boldsymbol{y}_0} \boldsymbol{c}(\boldsymbol{\alpha}-\boldsymbol{\gamma}/N+\boldsymbol{m}+i\boldsymbol{Q}'\boldsymbol{v})}{\rho - \boldsymbol{c}(\boldsymbol{\alpha}-\boldsymbol{\gamma}/N+i\boldsymbol{Q}'\boldsymbol{v})}\, d\boldsymbol{v}\, dt \\
&= \sum_{\boldsymbol{m}} \binom{\gamma}{\boldsymbol{m}} e^{m_1\boldsymbol{q}_1'\boldsymbol{y}_0/N+\cdots+m_N\boldsymbol{q}_N'\boldsymbol{y}_0/N} \int \frac{\mathscr{G}_\gamma^N(\boldsymbol{v}) e^{i\boldsymbol{v}'\boldsymbol{Q}\boldsymbol{y}_0} \boldsymbol{c}(\boldsymbol{\alpha}-\boldsymbol{\gamma}/N+\boldsymbol{m}+i\boldsymbol{Q}'\boldsymbol{v})}{\rho - \boldsymbol{c}(\boldsymbol{\alpha}-\boldsymbol{\gamma}/N+i\boldsymbol{Q}'\boldsymbol{v})}\, d\boldsymbol{v}\, dt\,.
\end{aligned}$$

We then get expected capital gains by dividing through by the price-dividend ratio, calculated above. The other component of expected return is the dividend yield, which is the reciprocal of the price-dividend ratio.

E.5 Interest rates

The price of a time-T zero-coupon bond is

$$B_T = \mathbb{E} e^{-\rho T} \left(\frac{C_T}{C_0}\right)^{-\gamma}\,.$$

Using the expectation calculated in section E.2, we have

$$\begin{aligned}
B_T &= e^{-\rho T} C_0^\gamma\, \mathbb{E} \frac{1}{(e^{y_{10}+\widetilde{y}_{1T}} + \cdots + e^{y_{N0}+\widetilde{y}_{NT}})^\gamma} \\
&= e^{-\rho T} \left(e^{\boldsymbol{q}_1'\boldsymbol{y}_0/N} + \cdots + e^{\boldsymbol{q}_N'\boldsymbol{y}_0/N}\right)^\gamma \int \mathscr{G}_\gamma^N(\boldsymbol{v}) e^{i\boldsymbol{v}'\boldsymbol{Q}\boldsymbol{y}_0} e^{\boldsymbol{c}(-\boldsymbol{\gamma}/N+i\boldsymbol{Q}'\boldsymbol{v})T}\, d\boldsymbol{v}\,.
\end{aligned}$$

The yield $\mathscr{Y}(T) = -(\log B_T)/T$. Using the above expression,

$$\mathscr{Y}(T) = \rho - \frac{1}{T} \log \left\{ \left(e^{\boldsymbol{q}_1'\boldsymbol{y}_0/N} + \cdots + e^{\boldsymbol{q}_N'\boldsymbol{y}_0/N}\right)^\gamma \int \mathscr{G}_\gamma^N(\boldsymbol{v}) e^{i\boldsymbol{v}'\boldsymbol{Q}\boldsymbol{y}_0} e^{\boldsymbol{c}(-\boldsymbol{\gamma}/N+i\boldsymbol{Q}'\boldsymbol{v})T}\, d\boldsymbol{v} \right\}\,.$$

To calculate the riskless rate, rearrange this expression slightly, using (57)—

$$\mathscr{Y}(T) = \rho - \frac{1}{T} \log \left\{ 1 + \left(e^{\boldsymbol{q}_1'\boldsymbol{y}_0/N} + \cdots + e^{\boldsymbol{q}_N'\boldsymbol{y}_0/N}\right)^\gamma \int \mathscr{G}_\gamma^N(\boldsymbol{v}) e^{i\boldsymbol{v}'\boldsymbol{Q}\boldsymbol{y}_0} \left(e^{\boldsymbol{c}(-\boldsymbol{\gamma}/N+i\boldsymbol{Q}'\boldsymbol{v})T} - 1\right)\, d\boldsymbol{v} \right\}\,.$$

Using L'Hôpital's rule, as in the two-tree case, we have

$$\begin{aligned} r &= \lim_{T\downarrow 0} \mathscr{Y}(T) \\ &= \rho - \left(e^{\boldsymbol{q}_1'\boldsymbol{y}_0/N} + \cdots + e^{\boldsymbol{q}_N'\boldsymbol{y}_0/N}\right)^\gamma \int \mathscr{G}_\gamma^N(\boldsymbol{v}) e^{i\boldsymbol{v}'\boldsymbol{Q}\boldsymbol{y}_0} \boldsymbol{c}(-\boldsymbol{\gamma}/N + i\boldsymbol{Q}'\boldsymbol{v})\, d\boldsymbol{v} \\ &= \left(e^{\boldsymbol{q}_1'\boldsymbol{y}_0/N} + \cdots + e^{\boldsymbol{q}_N'\boldsymbol{y}_0/N}\right)^\gamma \int \mathscr{G}_\gamma^N(\boldsymbol{v}) e^{i\boldsymbol{v}'\boldsymbol{Q}\boldsymbol{y}_0} \left[\rho - \boldsymbol{c}(-\boldsymbol{\gamma}/N + i\boldsymbol{Q}'\boldsymbol{v})\right] d\boldsymbol{v}\,. \end{aligned}$$

E.6 A final change of variables

The expressions so far obtained can be simplified by a final change of variables. Define $\widehat{\boldsymbol{v}} \equiv \boldsymbol{B}\boldsymbol{v}$, where $\boldsymbol{B}$ is the $(N-1)\times(N-1)$ square matrix

$$\boldsymbol{B} \equiv \begin{pmatrix} N-1 & -1 & \cdots & -1 \\ -1 & N-1 & \ddots & \vdots \\ \vdots & \ddots & \ddots & -1 \\ -1 & \cdots & -1 & N-1 \end{pmatrix}.$$

With this definition, we have $\widehat{v}_k = Nv_k - v_1 - \cdots - v_{N-1}$ and $\widehat{v}_1 + \cdots + \widehat{v}_{N-1} = v_1 + \cdots + v_{N-1}$. It is simple to verify that

$$\boldsymbol{B}^{-1} = \frac{1}{N} \begin{pmatrix} 2 & 1 & \cdots & 1 \\ 1 & 2 & \ddots & \vdots \\ \vdots & \ddots & \ddots & 1 \\ 1 & \cdots & 1 & 2 \end{pmatrix}.$$

Using the matrix determinant lemma (Fact 1 above) it is easy to calculate the Jacobian: $\det \boldsymbol{B}^{-1} = 1/N^{N-2}$, so—since $\boldsymbol{v} = \boldsymbol{B}^{-1}\widehat{\boldsymbol{v}}$—$d\boldsymbol{v}$ is replaced by $d\widehat{\boldsymbol{v}}/N^{N-2}$. Next, $\widehat{\boldsymbol{v}}$ was defined in such a way that $\mathscr{G}_\gamma^N(\boldsymbol{v})$, defined in equation (56), is equal to $N^{N-2}\mathscr{F}_\gamma^N(\widehat{\boldsymbol{v}})$, defined in equation (20). Finally, noting that $\boldsymbol{B}^{-1}\boldsymbol{Q} = \boldsymbol{U}$ and $\boldsymbol{u} \equiv \boldsymbol{U}\boldsymbol{y}_0$, as defined in (21), we have $\boldsymbol{Q}'\boldsymbol{v} = \boldsymbol{Q}'\boldsymbol{B}^{-1}\widehat{\boldsymbol{v}} = \boldsymbol{U}'\widehat{\boldsymbol{v}}$ and $\boldsymbol{v}'\boldsymbol{Q}\boldsymbol{y}_0 = \widehat{\boldsymbol{v}}'\boldsymbol{U}\boldsymbol{y}_0 = \widehat{\boldsymbol{v}}'\boldsymbol{u} = \boldsymbol{u}'\widehat{\boldsymbol{v}}$. Proposition 9 follows after making these substitutions throughout the various integrals and dropping hats on the integration variables $\widehat{\boldsymbol{v}}$.